Molecular Biology of the Cell
Vol. 12, 3175–3190, October 2001

A Novel Mechanism for Localizing Membrane Proteins to Yeast *Trans*-Golgi Network Requires Function of Synaptojanin-like Protein

Seon-Ah Ha,* Jeremy T. Bunch,* Hiroko Hama,† Daryll B. DeWald,† and Steven F. Nothwehr*‡

*Division of Biological Sciences, University of Missouri, Columbia, Missouri 65211; and †Department of Biology, Utah State University, Logan, Utah 84322

Submitted April 9, 2001; Revised July 9, 2001; Accepted July 24, 2001
Monitoring Editor: Hugh R.B. Pelham

Localization of resident membrane proteins to the yeast *trans*-Golgi network (TGN) involves both their retrieval from a prevacuolar/endosomal compartment (PVC) and a "slow delivery" mechanism that inhibits their TGN-to-PVC transport. A screen for genes required for the slow delivery mechanism uncovered *INP53*, a gene encoding a phosphoinositide phosphatase. A retrieval-defective model TGN protein, A(F→A)-ALP, was transported to the vacuole in *inp53* mutants approximately threefold faster than in wild type. Inp53p appears to function in a process distinct from PVC retrieval because combining *inp53* with mutations that block retrieval resulted in a much stronger phenotype than either mutation alone. In *vps27* strains defective for both anterograde and retrograde transport out of the PVC, a loss of Inp53p function markedly accelerated the rate of transport of TGN residents A-ALP and Kex2p into the PVC. Inp53p function is cargo specific because a loss of Inp53p function had no effect on the rate of Vps10p transport to the PVC in *vps27* cells. The rate of early secretory pathway transport appeared to be unaffected in *inp53* mutants. Cell fractionation experiments suggested that Inp53p associates with Golgi or endosomal membranes. Taken together, these results suggest that a phosphoinositide signaling event regulates TGN-to-PVC transport of select cargo proteins.

INTRODUCTION

The organization of the secretory pathway requires that specific sets of membrane proteins be targeted to particular organelles. Thus, a major challenge for the cell is to properly localize the resident proteins of organelles while mediating transport of other proteins. Resident membrane proteins of the *trans*-Golgi network (TGN) in the yeast *Saccharomyces cerevisiae* are localized in a dynamic manner. The yeast TGN, also referred to as the late-Golgi, contains three integral membrane proteases involved in the processing of the mating pheromone α-factor: Kex1p, Kex2p, and dipeptidyl aminopeptidase (DPAP) A (Fuller *et al.*, 1988). In addition, the TGN contains the carboxypeptidase Y (CPY) sorting receptor Vps10p (Marcusson *et al.*, 1994; Cooper and Stevens, 1996). Vps10p is thought to bind to its ligand CPY in the TGN whereupon the receptor–ligand complex is transported via vesicles to a prevacuolar/endosomal compartment (PVC). At the PVC the ligand dissociates from the receptor and the receptor recycles back to the TGN. Like Vps10p, DPAP A and Kex2p are known to cycle between the TGN and PVC without visiting the plasma membrane (Cooper and Bussey, 1992; Roberts *et al.*, 1992; Wilcox *et al.*, 1992; Bryant and Stevens, 1997). Recent evidence suggests that they may also visit early endosomes and earlier regions of the Golgi as part of their cycling itinerary (Lewis *et al.*, 2000; Bensen *et al.*, 2001).

Recent studies have indicated that two independent mechanisms exist for localization of membrane proteins to the TGN. TGN resident proteins can be retrieved back to the TGN after having reached the PVC. Aromatic amino acid-based signals in the cytosolic domains of DPAP A, Vps10p, and Kex2p are essential for PVC-to-TGN transport (Wilcox *et al.*, 1992; Nothwehr *et al.*, 1993; Cooper and Stevens, 1996). In DPAP A this signal consists of an FXFXD motif in which both phenylalanines are absolutely required. The retrieval

‡ Corresponding author. E-mail address: nothwehrs@missouri.edu.

Abbreviations used: ALP, alkaline phosphatase; CEN, yeast centromere; CPY, carboxypeptidase Y; DPAP, dipeptidyl aminopeptidase; ER, endoplasmic reticulum; ORF, open reading frame; PtdIns, phosphatidylinositol; PtdIns(3)P, phosphatidylinositol (3)-phosphate; PtdIns(4)P, phosphatidylinositol (4)-phosphate; PtdIns(3,5)P_2, phosphatidylinositol (3,5)-bisphosphate; PtdIns(4,5)P_2, phosphatidylinositol (4,5)-bisphosphate; PVC, prevacuolar/endosomal compartment; TGN, *trans*-Golgi network.

Table 1. Plasmids used in this study

Plasmid	Description	Reference or source
pRS316	CEN-*URA3* parental plasmid (no insert)	Sikorski and Hieter, 1989
pSN55	pRS316 containing *STE13-PHO8* gene fusion encoding A-ALP	Nothwehr *et al.*, 1993
pSN100	pRS316 containing *STE13-PHO8* gene fusion encoding A-ALP with $F_{85}A$ and $F_{87}A$ mutations	Nothwehr *et al.*, 1993
pAH97	pRS316 containing *GAL1* promoter-driven *STE13-PHO8* gene fusion encoding A-ALP with $F_{85}A$ and $F_{87}A$ mutations	This study
pAH16	CEN-*TRP1* plasmid containing *STE13-PHO8* gene fusion encoding A-ALP	Nothwehr *et al.*, 1999
pAH72	CEN-*TRP1* plasmid containing *STE13-PHO8* gene fusion encoding A-ALP with a deletion of residues 2–11	This study
pAH73	CEN-*TRP1* plasmid containing *STE13-PHO8* gene fusion encoding A-ALP with $F_{85}A$ and $F_{87}A$ mutations	This study
pSN124	CEN-*HIS3* plasmid containing *PHO8* gene	This study
pCWKX11	CEN-*URA3* plasmid containing *KEX2* gene with $Y_{713}A$ mutation	Wilcox *et al.*, 1992
p27	CEN-*URA3* plasmid containing approximately nucleotide 517,100 to 530,150 of *S. cerevisiae* chromosome 15	This study
pSH12	pRS316 containing *INP53* gene	This study
pSH14	pRS316 containing *inp53*Δ::*LEU2* allele	This study
pSH17	pRS316 containing *inp53-1* allele	This study
pSH18	*URA3*-based yeast integrating plasmid containing *inp53-1* allele	This study

mechanism appears to be vesicle mediated and requires a multimeric protein complex called the retromer complex (Horazdovsky *et al.*, 1997; Nothwehr and Hindes, 1997; Seaman *et al.*, 1998). The retromer complex appears to be a vesicle coat involved in formation of vesicles from the PVC. Indeed, genetic and biochemical evidence indicated that one of the retromer subunits (Vps35p) binds to the cytosolic domains of DPAP A and Vps10p via interaction with the retrieval signals (Nothwehr *et al.*, 1999, 2000).

A second mechanism exists to ensure that DPAP A and Kex2p are transported from the TGN to the PVC at a slow rate. This mechanism, referred to in this report as the "slow delivery" mechanism, was originally observed with the use of a class E yeast mutant in which anterograde TGN-to-PVC traffic occurs normally but both anterograde and retrograde transport out of the PVC are blocked (Bryant and Stevens, 1997). In such mutants, a model TGN resident membrane protein containing the DPAP A cytosolic domain (A-ALP) was transported to the PVC very slowly compared with the rapid rate of TGN-to-PVC transport exhibited by Vps10p. A region of the DPAP A cytosolic domain distinct from the FXFXD retrieval motif was necessary for the slow delivery mechanism. Mutations within this region caused A-ALP to be delivered to the PVC with a rate similar to that of Vps10p. In contrast to the retrieval mechanism, the *cis*-acting information required for slow delivery is poorly defined and the machinery that mediates this process is unknown.

With the use of a screen designed to identify mutants defective in the slow delivery mechanism for TGN localization, we have identified a mutant carrying a novel allele of the *INP53* gene. *INP53* encodes a synaptojanin-like protein that contains a SAC1-like domain encoding a polyphosphoinositide phosphatase and a domain encoding a phosphoinositide 5-phosphatase (Guo *et al.*, 1999; Hughes *et al.*, 2000b). Loss of Inp53p increases the rate of TGN-to-PVC delivery of A-ALP and Kex2p but does not affect their retrieval from the PVC. Furthermore, TGN/PVC cycling of Vps10p, which does not exhibit slow delivery into the PVC, is unaffected by a loss of Inp53p. Thus, Inp53p appears to play a very specific role in regulating the rate of TGN-to-PVC trafficking of certain cargo.

MATERIALS AND METHODS

Antibodies

Rabbit polyclonal antibodies against alkaline phosphatase (ALP) (Nothwehr *et al.*, 1996) and Kex2p (Spelbrink and Nothwehr, 1999) have been previously described. The Vps10p and phosphoglycerol kinase rabbit polyclonal antibodies were gifts from T. Stevens (University of Oregon, Eugene, OR). Rabbit polyclonal antibodies against CPY and α-factor were gifts from S. Emr (University of California, San Diego, La Jolla, CA) and G. Payne (University of California, Los Angeles, Los Angeles, CA), respectively. The mouse Vph1p and mouse Vma2p (monoclonal antibody 13D11-B2) antibodies were from Molecular Probes (Eugene, OR). Finally, all secondary antibodies and streptavidin conjugated to fluorescein isothiocyanate (FITC) for immunofluorescence experiments were obtained from Jackson Immunoresearch (West Grove, PA).

Rabbit antibodies were raised against the product of the *INP53* gene. A plasmid expressing amino acids 784-1096 of Inp53p fused to a 6xHis tag was constructed by subcloning the 936-bp AseI-*Nde*I fragment from the *INP53* gene into the *Nde*I site of pET28(a)+ (Novagen, Madison, WI). Induction of *Escherichia coli* carrying the resulting plasmid (pJB11) with isopropyl-1-β-D-thiogalactopyranoside produced a fusion protein that was purified with the use of a Ni-nitrilotetraacetic acid-agarose column (QIAGEN, Valencia, CA). Antibodies were raised against the purified protein in New Zealand White rabbits.

Mutant Screen and Cloning of GRD21/INP53

The *MAT*α parental strain LSY7 (Table 1) carrying A(F→A)-ALP in the genome was mutagenized by ethyl methanesulfonate as previously described (Nothwehr *et al.*, 1996). A total of 37,000 mutagenized colonies was screened at a density of 1,000 colonies per plate with the use of the ALP activity assay (Chapman and Munro, 1994; Nothwehr *et al.*, 1996). Clones consistently exhibiting elevated ALP activity were further assessed for proteolytic processing of A(F→A)-ALP, CPY secretion, and pro-α-factor secretion. Mutants that secreted CPY were used for complementation analysis with *vps* and *grd* mutant collections (Robinson *et al.*, 1988; Raymond *et al.*,

Table 2. *S. cerevisiae* strains used in this study

Strain	Description	Source or reference
SEY6210	*MATα leu2-3,112 ura3-52 his3-Δ200 trp1-Δ901 lys2-801 suc2-Δ9*	Robinson *et al.*, 1988
LSY7	*MATα leu2-3,112 ura3-52 his3-Δ200 trp1-Δ901 lys2-801 suc2-Δ9 pho8::ste13($F_{85}A$; $F_{87}A$)-pho8*	This study
SNY17	*MATα leu2-3,112 ura3-52 his3-Δ200 trp1-Δ901 lys2-801 suc2-Δ9 pho8Δ::LEU2*	Nothwehr *et al.*, 1985
SNY79	*MATα leu2-3,112 ura3-52 his3-Δ200 trp1-Δ901 lys2-801 suc2-Δ9 pho8Δ::LEU2 vps35Δ::HIS3*	Nothwehr *et al.*, 1999
SHY35	*MATα leu2-3,112 ura3-52 his3-Δ200 trp1-Δ901 suc2-Δ9 pho8Δ::ADE2*	This study
SHY38	*MATα leu2-3,112 ura3-52 his3-Δ200 trp1-Δ901 suc2-Δ9 pho8Δ::ADE2 inp53Δ::LEU2*	This study
SHY40	*MATα leu2-3,112 ura3-52 his3-Δ200 trp1-Δ901 suc2-Δ9 pho8Δ::ADE2 inp53-1*	This study
SHY42	*MATα leu2-3,112 ura3-52 his3-Δ200 trp1-Δ901 suc2-Δ9 pho8Δ::ADE2 vps27Δ::LEU2*	This study
SHY43	*MATα leu2-3,112 ura3-52 his3-Δ200 trp1-Δ901 suc2-Δ9 pho8Δ::ADE2 vps27Δ::LEU2 inp53-1*	This study
SHY44	*MATα leu2-3,112 ura3-52 his3-Δ200 trp1-Δ901 suc2-Δ9 pho8Δ::ADE2 kex2Δ::LEU2*	This study
SHY45	*MATα leu2-3,112 ura3-52 his3-Δ200 trp1-Δ901 suc2-Δ9 pho8Δ::ADE2 kex2Δ::LEU2 inp53-1*	This study
SHY50-3B	*MATα leu2-3,112 ura3-52 his3-Δ200 trp1-Δ901 suc2-Δ9 pho8Δ::ADE2 inp53-1 pep4Δ::LEU2*	This study
W303-1a	*MAT***a** *ura3-1 leu2-3,112 his3-11,15 trp1-1 ade2-1 can1-100*	R. Rothstein
AHY62	*MAT***a** *ura3-1 leu2-3,112 his3-11,15 trp1-1 ade2-1 can1-100 pho8Δ::ADE2 pep4Δ::TRP1*	This study
SHY37-2C	*MATα ura3 leu2-3,112 his3 trp1 (ade2-1 or ADE2) (CAN1 or can1-100) pho8Δ::ADE2 pep4Δ::TRP1 inp53-1*	This study

Strains LSY7, SNY17, and SNY79 were derived from parent strain SEY6210. Strains SHY38–SHY45 were derived from parent strain SHY35. AHY62 was derived from W303-1a. SHY37-2C was made by crossing LSY7, containing an *inp53-1* allele, with a W303-1a–derived strain followed by sporulation and repeated backcrossing of the progeny with a W303-1a–derived strain.

1992; Nothwehr *et al.*, 1996). Mutants chosen for further analyses were backcrossed against the parental wild-type strain of the opposite mating type, sporulated, and the resulting tetrads were analyzed for linkage of the *grd* phenotype with a single mutation. A plasmid from a YCp50-based yeast genomic library (Rose *et al.*, 1987) called p27 was found that complemented the *grd* phenotype of yeast mutant *grd21*. Further analysis showed that the open reading frame (ORF) *YOR109w/INP53/SOP2/SJL3* was sufficient for complementation.

Construction of Plasmids and Yeast Strains

Most of the plasmids and yeast strains used in this study are described in Tables 1 and 2, respectively. A centromeric (CEN) plasmid called pSH12 containing the *INP53* gene was constructed by subcloning a 5.6-kbp *Xba*I fragment from p27 into the *Xba*I site of pRS316 (Sikorski and Hieter, 1989). The *inp53-1* allele was rescued from the genome by transforming an *inp53-1* yeast strain with pSH12 lacking the *Nhe*I-AatII fragment containing the *INP53* ORF. The resulting gap-repaired plasmid was then isolated from Ura^+ transformants, resulting in pSH17. A vector for integrating the *inp53-1* allele into the *INP53* locus was constructed by subcloning the 5.67-kbp *Xba*I fragment from pSH17 into the *Xba*I site of pRS306, resulting in pSH18. Construction of a *inp53Δ::LEU2* knockout construct was performed by subcloning a 2488-bp AatII-*Xba*I fragment containing the *LEU2* gene into the AatII/*Nhe*I sites of pSH12. This removed all but the final 112 nucleotides of the 3324 nucleotide *INP53* ORF. pSN124 is equivalent to pSN92 (Nothwehr *et al.*, 1993), except it is derived from pRS313 rather than pRS316.

To construct yeast strain LSY7, the pRS306-derived plasmid pLS10 was made that contained the following insert segments fused together in the following order (the first nucleotide of each ORF is defined as +1): nucleotides −989 to −161 of the *PHO8* gene, nucleotides −1584 to +352 of the *STE13* gene (containing $F_{85}A$ and $F_{87}A$ mutations), and nucleotides +88 to +1924 of the *PHO8* gene. This plasmid was digested with *Sac*I and transformed into yeast strain SEY6210 to target the construct to the *PHO8* locus. Ura^+ transformants were then grown on media containing 5-fluoroorotic acid to select for Ura^- loop-outs. Ura^- strains were then screened by Western blot for the presence of the integrated A(F→A)-ALP construct.

The mating type of yeast strain SNY36-9A (Nothwehr *et al.*, 1995) was switched to *MATα* by transforming it with a plasmid expressing the homothallic switching endonuclease. The resulting *MATα* strain was cured of the plasmid, resulting in strain SHY35. To introduce the *inp53Δ::LEU2* allele into SHY35, it was transformed with the 4.3-kbp *Bam*HI fragment from pSH14. Leu^+ transformants were then screened for the *inp53Δ::LEU2* mutation by polymerase chain reaction analysis. Introduction of the *inp53-1* mutation into SHY35 was accomplished by transforming it with pSH18 digested with *Bgl*II. Ura^+ transformants were grown on media containing 5-fluoroorotic acid to select for Ura^- loop-outs. Ura^- strains were then screened for the pro-α-factor secretion phenotype, resulting in strain SHY40.

Radiolabeling, Immunoprecipitation, and Subcellular Fractionation

Yeast strains were propagated at 30°C for all pulse-chase experiments. The procedure for immunoprecipitation of CPY has been previously described (Vater *et al.*, 1992). The procedure for immunoprecipitation of Vps10p, Kex2p, ALP, and A-ALP was performed as previously described (Nothwehr *et al.*, 1993). Radioactively labeled proteins were quantified from gels with the use of a PhosphorImager system (Fuji Photo Film, Tokyo, Japan). The half-time of Kex2p turnover was determined by calculating the percentage of protein remaining at a given time point compared with that present at the 0-min time point. Linear regression analysis was then carried out on plots of the log of the percentage of protein remaining as a function of time. For calculation of the half-time of wild-type and mutant A-ALP processing, the log of the percentage of A-ALP that was unprocessed at each time point was plotted as a function of time, and the plots were analyzed by linear regression analysis. In experiments in which a significant amount of the mature form of wild-type or mutant A-ALP was degraded to a proteolytic fragment (Figure 1A), the amount of the proteolytic fragment was included in the calculation of total A-ALP present.

The subcellular fractionation experiment shown in Figure 6B was carried out as previously described (Nothwehr *et al.*, 1999), except that the immunoprecipitations were performed with the use of anti-Vps10p antibody rather than anti-Vps35p.

The subcellular fractionation experiment carried out in Figure 9 was performed by harvesting 50 OD_{600} units of yeast cells growing in mid-log phase, washing them with 50 ml of dH_2O, and sphero-

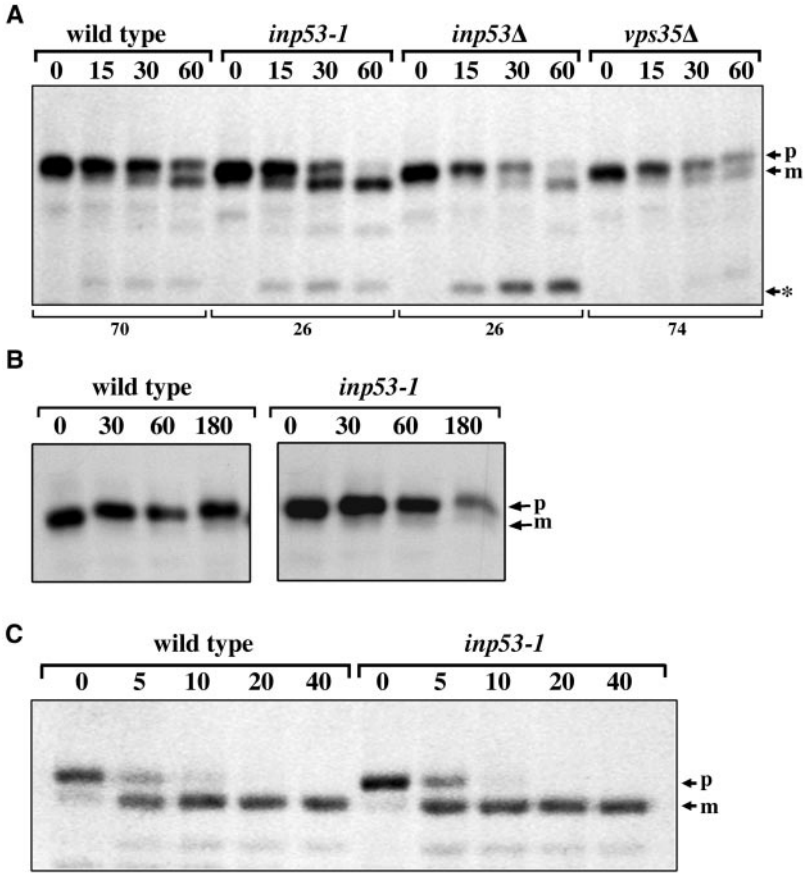

Figure 1. A(F→A)-ALP exhibits more rapid vacuolar processing in *inp53* mutants than in wild-type. Cells were pulsed with [^{35}S]methionine/cysteine for 10 min. Unlabeled amino acids were then added to initiate the chase at the times (min) indicated above each panel. (A) A(F→A)-ALP was immunoprecipitated from the cultures and was analyzed by SDS-PAGE and fluorography. Wild-type (SHY35), *inp53-1* (SHY40), *inp53*Δ (SHY38), and *vps35*Δ (SNY79) yeast strains carrying a plasmid directing expression of A(F→A)-ALP (pAH73) were analyzed. The half-time of A(F→A)-ALP processing is indicated beneath the panel for each strain. (B) Wild-type A-ALP was immunoprecipitated and analyzed as in A. Wild-type (SHY35) and *inp53-1* (SHY40) yeast strains carrying plasmid pAH16 were analyzed. (C) ALP was immunoprecipitated from SHY35 and SHY40 cells and analyzed as in A. The positions of wild-type or mutant A-ALP and ALP precursor (p) and mature/processed (m) forms are indicated, as well as a proteolytic breakdown product (*) in A.

plasting them in 14.5 ml of 1.4 M sorbitol, 50 mM Tris pH 7.5, 2 mM $MgCl_2$, and 10 mM NaN_3 containing 0.16 mg of oxalyticase (Enzogenetics, Corvallis, OR) for 45 min at 30°C. The spheroplasts were washed with 10 ml of ice-cold 1.2 M sorbitol, 5 mM NaN_3 and were resuspended in 10 ml of ice-cold lysis buffer (25 mM sodium phosphate pH 7.4, 200 mM mannitol, 1 mM EGTA, and 5 mM $MgCl_2$) containing freshly added protease inhibitors (0.5 mM phenylmethylsulfonyl fluoride, 1 μg/ml leupeptin, and 1 μg/ml pepstatin A). The resulting lysate was centrifuged at 460 × *g* for 12 min to pellet unlysed cells. The supernatant was then centrifuged at 15,000 × *g* for 15 min to create pellet (P15) and supernatant (S15) fractions. The S15 fraction was then centrifuged at 200,000 × *g* for 2 h to generate pellet (P200) and supernatant (S200) fractions. The P15, P200, and S200 fractions were separated by SDS-PAGE, electroblotted, and the blots probed with antibodies against Vph1p, Kex2p, phosphoglycerol kinase, and Inp53p. After subsequent incubation with alkaline phosphatase-conjugated secondary antibodies, the blots were developed with the use of Lumi-Phos substrate (Pierce, Rockford, IL) and imaged with the use of a LAS-1000 luminescent image analyzer (Fuji Photo Film) and Adobe Photoshop 5.5 software (Adobe Systems, Mountain View, CA).

Fluorescence Microscopy

For induction of A(F→A)-ALP synthesis in yeast strains via the *GAL1* promoter before analysis by fluorescence microscopy, strains were propagated overnight in minimal media containing 2% (wt/vol) raffinose. Log-phase cultures were then adjusted to 2% galactose to induce expression. After 40 min of induction, cultures were adjusted to 2% glucose to shut off expression, and aliquots of 10 ml were removed at 0, 15, 30, and 60-min time points and fixed by addition of 1.2 ml of 37% formaldehyde.

The procedures for preparation of fixed spheroplasted yeast cells and attachment to microscope slides were previously described (Roberts *et al.*, 1991). All secondary antibodies were diluted 1:500 before use.

Simultaneous detection of A(F→A)-ALP and Vma2p was carried out by incubating with the following reagents followed by extensive washing: 1) rabbit anti-ALP and mouse anti-Vma2p antibodies, 2) biotin-conjugated goat anti-rabbit IgG (H + L), 3) FITC-streptavidin and Texas Red-conjugated goat anti-mouse IgG (H + L). Simultaneous detection of Kex2p and Vma2p was carried out the same way except rabbit anti-Kex2p antibody replaced the anti-ALP antibody.

To quantify the percentage of cells exhibiting vacuolar staining of A(F→A)-ALP 100–150 randomly selected cells were analyzed for each time point. Cells exhibiting prominent vacuolar membrane staining regardless of any other staining pattern were included in the percentage value. Yeast cells were photographed with the use of an Olympus BX-60 fluorescence microscope (Olympus, Lake Success, NY). Film negatives were digitized with the use of a Kodak Professional RFS 2035 Plus film scanner and processed into figures with the use of Adobe Photoshop 5.5.

Phosphoinositide Analysis

The phosphoinositide analyses were performed essentially as described previously (Hama *et al.*, 2000). Yeast strains were grown at 30°C to an OD_{600} of between 0.6 and 0.8 in 10 ml of standard SD medium (without supplemental inositol) plus 5 μCi/ml [^{3}H]myo-inositol (16 Ci/mmol; Amersham Pharmacia Biotech, Arlington

Heights, IL). Growth was terminated by addition of trichloroacetic acid to a final concentration of 5% (wt/vol) followed by incubation on ice for 1 h. Cells were washed with H_2O and suspended in 0.5 ml of H_2O. Lipids were extracted as described (Hanson and Lester, 1980) by combining the cells with 0.7 ml of 95% ethanol/diethyl ether/pyridine/ammonium hydroxide (15:5:1:0.018) and extracting at 57°C for 30 min. Cell debris was removed by centrifugation and the supernatant was dried under N_2.

Lipids were deacylated as previously described (Serunian *et al.*, 1991) with minor modifications. Dried lipids were resuspended in 0.5 ml of methylamine reagent (42.8% of 25% methylamine, 45.7% of methanol, 11.4% of *n*-butanol) by bath sonication, incubated at 53°C for 50 min, and dried in vacuo. Deacylated lipids were suspended in 0.5 ml of H_2O by sonication and then extracted three times with 0.5 ml of *n*-butanol/petroleum ether/ethyl formate (20:4:1). The aqueous phase was dried in vacuo, and suspended in a small volume of H_2O for high-performance liquid chromatography (HPLC) analysis.

Glycerophosphoinositol species were resolved with the use of anion exchange chromatography with a Partisil 10 SAX (4.6 × 250 mm) column and a Beckman System Gold chromatograph. For each sample, equivalent counts were loaded (2.5×10^6 cpm). Fractions were collected every 0.3 min, mixed with 2–3 ml of EcoLume (ICN, Costa Mesa, CA), and counted in a liquid scintillation counter (Beckman LS 5801). Glycerophosphoinositol phosphate species eluted at identical times as previously chromatographed standards (Hama *et al.*, 2000).

RESULTS

Genetic Screen to Identify Mutants Defective in Slow Delivery of TGN Protein to PVC

A-ALP is a model TGN-membrane protein consisting of the N-terminal cytosolic domain of DPAP A, the *STE13* gene product, fused to the transmembrane and lumenal domains of ALP, the *PHO8* gene product (Nothwehr *et al.*, 1993). A failure to retain A-ALP in the TGN results in its delivery to the vacuole where its C-terminal propeptide is proteolytically removed. Propeptide removal activates A-ALP, thus its mislocalization to the vacuole can be assayed by the increase in alkaline phosphatase activity. To identify genes required for maintaining the slow rate of delivery of A-ALP into the PVC we used a mutant form of A-ALP in which both phenylalanines of the $FXFXD_{89}$ retrieval motif were mutated to alanines. This mutant, called A(F→A)-ALP, is not retrieved from the PVC and is transported to the vacuole with a half-time of 60–70 min (Nothwehr *et al.*, 1993; Bryant and Stevens, 1997). We reasoned that A(F→A)-ALP would be a useful reporter for identification of mutants defective in slow delivery because the only mechanism preventing its rapid delivery to the vacuole was the slow delivery mechanism. Such mutants would exhibit a more rapid rate of A(F→A)-ALP vacuolar delivery and a somewhat higher steady-state level of its activity.

Yeast cells in which the chromosomal copy of the *PHO8* gene was replaced with a fusion construct expressing A(F→A)-ALP were mutagenized with ethyl methanesulfonate. Out of 37,000 mutants screened in the LSY7 strain background a total of 120 mutants exhibiting elevated A(F→A)-ALP activity was identified with the use of a colorimetric assay (Chapman and Munro, 1994; Nothwehr *et al.*, 1996). The rate of A(F→A)-ALP vacuolar processing was then analyzed in 60 of these mutants, resulting in two mutants that clearly exhibited more rapid processing than wild-type. Genetic analysis demonstrated that the phenotype of each mutant was due to a single recessive mutation and that the mutants represented distinct complementation groups that were named *grd21* and *grd22*. The *grd21* mutant was chosen for further analysis because of its stronger processing phenotype. *MATα grd21* strains were found to secrete unprocessed pro-α-factor but exhibited no CPY missorting defects (see below). Plasmids were identified from a CEN plasmid-based yeast genomic library (Rose *et al.*, 1987) that complemented the pro-α-factor secretion phenotype. Analysis of the plasmids demonstrated that the *YOR109w/INP53/SOP2/SJL3* gene was necessary and sufficient for complementation. Genetic analysis showed that the *grd21* mutation was tightly linked to the *YOR109w* locus. We will hereafter refer to this gene as *INP53* and the *grd21* mutant allele as *inp53-1*. A mutant yeast strain containing a deletion of nearly the entire *INP53* open reading frame exhibited no detectable growth defects (our unpublished results), consistent with earlier studies (Srinivasan *et al.*, 1997; Singer-Krüger *et al.*, 1998; Stolz *et al.*, 1998).

Retrieval-defective A-ALP Mutant Is Transported to Vacuole More Rapidly in inp53 Cells Than in Wild-Type

To compare wild-type, *inp53-1*, and *inp53*Δ cells for the rate of transport of A(F→A)-ALP to the vacuole, we analyzed the rate of its vacuolar processing. Processing was analyzed by pulse labeling cells with [^{35}S]methionine/cysteine for 10 min, chasing for the indicated times, and immunoprecipitating A(F→A)-ALP (Figure 1A). Consistent with previous reports (Nothwehr *et al.*, 1993, 1999), A(F→A)-ALP was processed with a half-time of 70 min in wild-type cells. In the *inp53-1* and *inp53*Δ strains vacuolar processing occurred much more rapidly with a half-time of 26 min in both cases. In contrast, in a *vps35*Δ mutant with a specific defect in PVC-to-TGN retrieval A(F→A)-ALP was processed at the same rate as in wild type. The lack of an additional defect on A(F→A)-ALP mislocalization to the vacuole due to the *vps35*Δ mutation is consistent with the idea that the $F_{85}A$ and $F_{87}A$ mutations have rendered the protein completely defective for retrieval. These data are also consistent with the idea that the trafficking defect in the *inp53* mutant cells is distinct from the PVC-to-TGN retrieval step. The rate of processing of A(F→A)-ALP was similar for the *inp53-1* and *inp53*Δ strains; however, the *inp53*Δ strain exhibited an abnormally high degree of proteolysis of the mature A(F→A)-ALP form to a smaller product. The presence of this breakdown product was taken into account when the processing half-time was calculated (see MATERIALS AND METHODS). Proteolysis of mature A(F→A)-ALP apparently occurs in the vacuole, because it is dependent on vacuolar proteases (our unpublished results). The basis of this difference in proteolysis of the *inp53*Δ mutant is not known.

The effect of a loss of Inp53p function on localization of wild-type A-ALP was also assessed (Figure 1B). Very little A-ALP was mislocalized to the vacuole even after 180-min chase in the *inp53-1* strain. This near wild-type level of avoidance of vacuolar delivery suggests that the retrieval mechanism is highly efficient for A-ALP and can prevent extensive vacuolar mislocalization in the absence of the slow delivery mechanism.

As a test of the specificity of Inp53p function, we assessed the rate of transport of the vacuolar membrane protein ALP

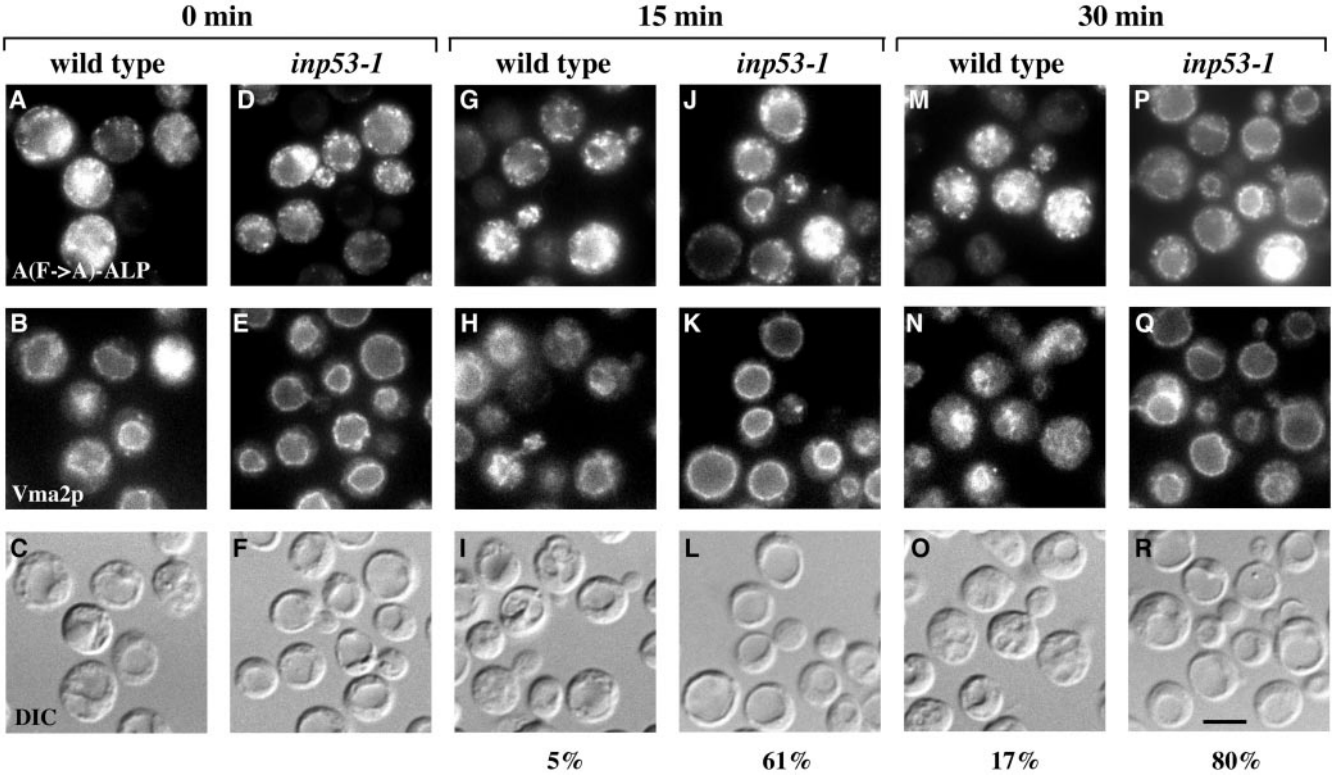

Figure 2. A(F→A)-ALP is delivered to the vacuole more rapidly in the *inp53-1* mutant than in wild type. Wild-type (AHY62) and *inp53-1* (SHY37-2C) strains carrying plasmid containing a *GAL1* promoter-driven A(F→A)-ALP construct (pAH97) were propagated for several doublings in media containing raffinose followed by growth in galactose media for 40 min to induce A(F→A)-ALP expression. Glucose was then added (0-min time point) to shut off expression, and aliquots of cells were fixed at the indicated time points. The cells were then spheroplasted and costained for A(F→A)-ALP and Vma2p. After subsequent treatment with fluorochrome-conjugated secondary antibodies, the cells were viewed by differential interference contrast optics and by epifluorescence through filters specific for FITC and Texas Red. The percentage of cells exhibiting vacuolar staining of A(F→A)-ALP (see MATERIALS AND METHODS) is indicated for each strain at the 15- and 30-min time points. Bar, 5 μm.

to the vacuole. ALP is packaged into vesicles at the TGN whose formation requires AP-3 adaptor subunits (Cowles *et al.*, 1997a). ALP is then transported to the vacuole via a pathway that bypasses the PVC (Cowles *et al.*, 1997b; Piper *et al.*, 1997). Wild-type and *inp53* mutant strains were pulsed, chased, and ALP was immunoprecipitated at various time points (Figure 1C). The rate of ALP trafficking to the vacuole was virtually identical in the two strains. These results indicate that Inp53p is not required for sorting into and trafficking within the ALP pathway for TGN-to-vacuole transport and does not regulate the rate of this process.

To further assess the defect in slow delivery observed in *inp53* mutants, the subcellular localization of a "wave" of newly expressed A(F→A)-ALP was examined by indirect immunofluorescence microscopy at various time points after synthesis. A gene fusion encoding A(F→A)-ALP was expressed under control of the regulatable *GAL1* promoter. Wild-type and *inp53-1* cells were propagated overnight in raffinose-containing media to repress A(F→A)-ALP expression. Expression was induced by adding galactose to the cultures, and 40 min later was shut off by adding glucose. At 0, 15, and 30 min after glucose addition cells were fixed and stained for A(F→A)-ALP and Vma2p, a vacuolar membrane marker (Figure 2). At the 0-min time point much of the A(F→A)-ALP staining pattern in both strains was perinuclear, consistent with endoplasmic reticulum (ER) localization. A punctate pattern was also observed for A(F→A)-ALP consistent with a Golgi distribution (Figure 2, A and D). At 15 min the wild-type strain exhibited a predominantly punctate, Golgi-like staining pattern (Figure 2G) with only 5% of the cells exhibiting vacuolar staining. In contrast, 61% of the *inp53-1* cells at the 15-min time point exhibited vacuolar membrane staining (Figure 2; compare J and K) as well as some punctate staining. At 30 min 17% of the wild-type and 80% of the *inp53-1* cells exhibited vacuolar staining. By 60 min virtually all of the cells from both strains exhibited vacuolar staining for A(F→A)-ALP (our unpublished results). These results, taken together with the processing results, indicate that A(F→A)-ALP reaches the vacuole more rapidly in the *inp53* mutant cells than in wild-type cells. In addition, loss of Inp53p function affected vacuole size, suggesting that Inp53p is required for proper vacuolar membrane homeostasis.

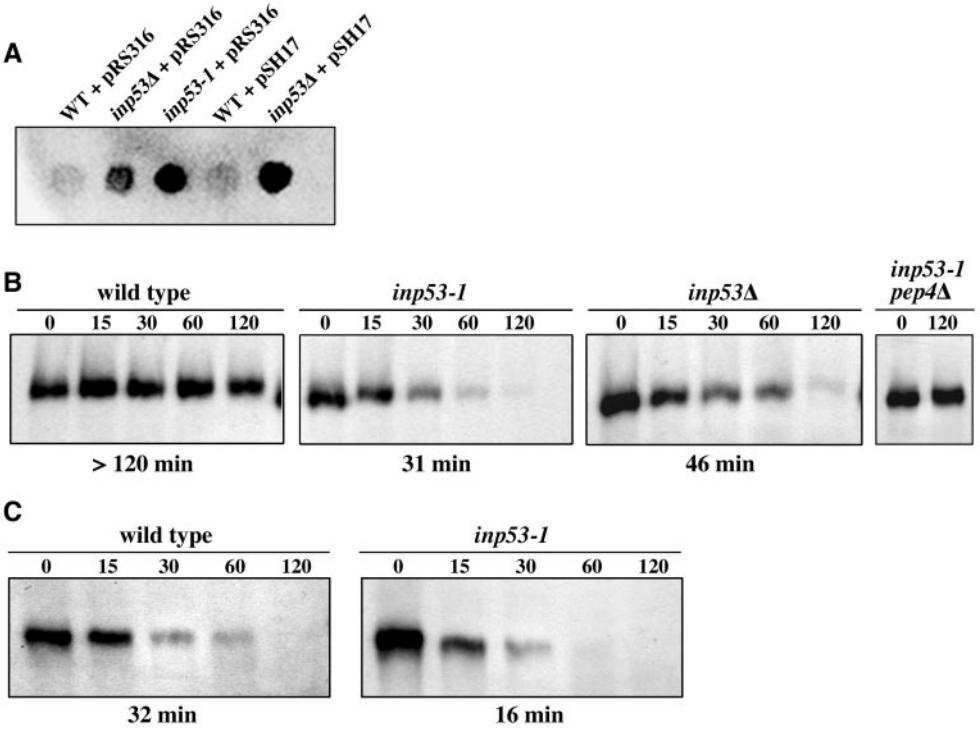

Figure 3. Localization and trafficking of Kex2p are affected in *inp53* mutants. (A) Immunoblot analysis of pro-α-factor secretion was performed on the following strain/plasmid combinations from left to right: SHY35/pRS316,SHY38/pRS316,SHY40/pRS316, SHY35/pSH17, and SHY38/pSH17. (B) Strains SHY35, SHY40, SHY38, and SHY50-3B were pulsed for 10 min with [^{35}S]methionine/cysteine before unlabeled amino acids were added to initiate the chase. Kex2p was immunoprecipitated from the cells at the indicated chase times. (C) Kex2p-Y_{713}A mutant was immunoprecipitated as in B from strains SHY44 and SHY45 transformed with plasmid pCWKX11. Half-time of Kex2p turnover is indicated below the panel for each strain in B and C. Values represent the mean of two experimental determinations that differed <7%.

Kex2p Localization to TGN Is Defective in inp53 Mutants

The Kex2p endoprotease is a type I membrane protein that is localized to the TGN, where it performs the initial processing event to convert the pro-α-factor pheromone to mature α-factor (Fuller *et al.*, 1988). A loss of Kex2p localization in the TGN results in secretion of unprocessed pro-α-factor rather than the mature form (Fuller *et al.*, 1989), and thus secretion of pro-α-factor serves as an assay for Kex2p localization. Kex2p, like DPAP A, is localized to the TGN in part via an aromatic amino acid-based sorting signal (called TLS1) in its cytosolic domain involved in PVC-to-TGN retrieval (Wilcox *et al.*, 1992; Brickner and Fuller, 1997). Kex2p contains a second cytoplasmic domain TGN localization signal (called TLS2) that does not appear to function in the retrieval step (Brickner and Fuller, 1997) and may be analogous in function to the slow delivery signal of A-ALP.

To determine whether Inp53p is involved in regulating TGN-to-PVC trafficking of Kex2p, localization and trafficking of Kex2p were assessed in *inp53* mutants. With the use of a colony-blotting approach, a modest pro-α-factor secretion defect was observed for the *inp53*Δ strain (Figure 3A), consistent with a previous study (Bensen *et al.*, 2000). However, a more robust defect was consistently observed for the *inp53-1* strain.

Loss of Kex2p localization in the TGN often causes it to be rapidly mislocalized and degraded in the vacuole. In the wild-type strain Kex2p was slowly degraded with a half-time of >120 min (Figure 3B), whereas in the *inp53-1* and *inp53*Δ mutants the half-time was substantially reduced to 31 and 46 min, respectively, consistent with the pro-α-factor secretion results. No degradation of Kex2p was observed in the *inp53-1* strain if the *PEP4* gene encoding a vacuolar protease was disrupted, indicating that turnover occurred within the vacuole. These results expand on a previous study showing that the steady-state levels of Kex2p were moderately reduced in an *inp53* mutant (Luo and Chang, 1997).

The subcellular localization of Kex2p was also assessed by indirect immunofluorescence microscopy in wild-type and *inp53-1* cells (Figure 4). Kex2p exhibits a nonvacuolar punctate staining appearance in wild-type cells typical of the morphology of the yeast TGN (Redding *et al.*, 1991; Roberts *et al.*, 1992). In contrast, Kex2p in *inp53-1* cells primarily exhibited staining in the vacuole. In some *inp53-1* cells Kex2p localized to the rim of the vacuole, whereas in other cases it exhibited a vacuolar lumen-staining pattern reminiscent of membrane proteins that are delivered to the vacuole via the multivesicular body pathway (Odorizzi *et al.*, 1998). Taken together, these results suggest that loss of Inp53p function compromises TGN localization of Kex2p.

To determine whether Inp53p was involved in a Kex2p localization mechanism distinct from the PVC retrieval mechanism we assessed whether Inp53p was required for the localization mediated by the TLS2 signal of Kex2p. The rate of vacuolar turnover of a mutant form of Kex2p (Kex2p-Y_{713}A) lacking TLS1 but retaining TLS2 was assessed in wild-type and *inp53-1* cells (Figure 3C). In *inp53-1* cells Y_{713}A Kex2p exhibited a markedly shorter half-time of turnover (16 min) than in wild-type cells (32 min). The additive affect of mutations in TLS1 and *INP53* suggests that Inp53p is required for TLS2 function in localization of Kex2p at a step distinct from the retrieval step.

Surprisingly, *inp53-1* strains reproducibly exhibited stronger pro-α-factor secretion and Kex2p turnover phenotypes than that of the *inp53*Δ strains (Figure 3, A and B). Such

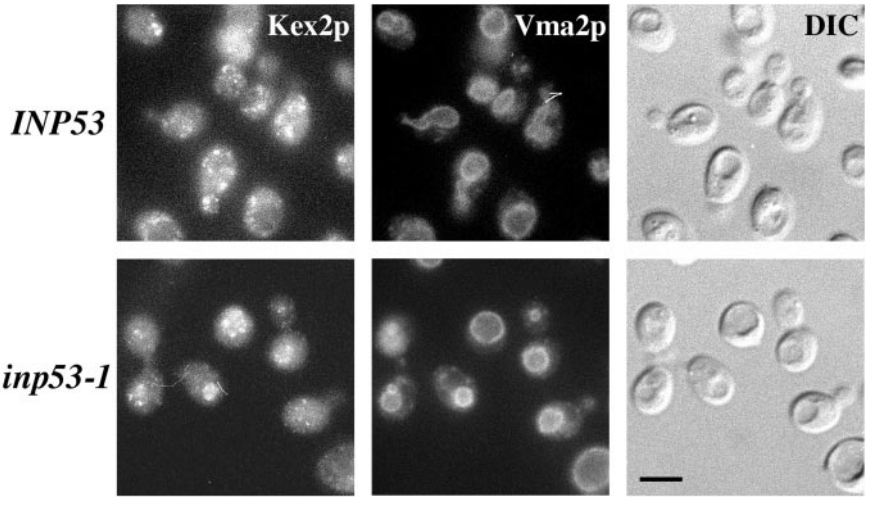

Figure 4. Kex2p is mislocalized to the vacuole in *inp53* mutants. Wild-type (AHY62) and *inp53-1* (SHY37-2C) cells were fixed, spheroplasted, and costained for Kex2p and Vma2p. After subsequent treatment with fluorochrome-conjugated secondary antibodies, cell images were collected as in Figure 2. Bar, 5 μm.

behavior is often characteristic of a dominant allele; however, our initial genetic studies of *inp53-1* suggested it was a recessive allele. To confirm this with the use of the pro-α-factor secretion phenotype, we rescued the *inp53-1* allele from yeast onto a CEN plasmid with the use of the gap repair technique (Orr-Weaver *et al.*, 1983). The presence of this plasmid (pSH17) did not cause an otherwise wild-type strain to secrete pro-α-factor demonstrating that *inp53-1* is, indeed, a recessive allele (Figure 3A). As expected, an *inp53*Δ strain carrying pSH17 secreted substantially more pro-α-factor than *inp53*Δ carrying an empty vector, thus pSH17 is functional. These results suggest that the *inp53-1* allele encodes a protein that interferes with Kex2p trafficking in the absence of wild-type Inp53p but not in its presence.

Rate of Golgi-to-PVC Transport of A-ALP and Kex2p Is Accelerated in inp53 Mutant Cells

The rapid delivery of newly synthesized A(F→A)-ALP to the vacuole in *inp53* cells could reflect an increase in the kinetics of Golgi-to-PVC transport or an increase in the rate of transport at another step. Class E *vps* mutants provide a means for assessing the rate of transport of newly synthesized proteins to the PVC (Bryant and Stevens, 1997). In such mutants transport from the TGN to the PVC occurs normally, but both retrograde and anterograde traffic out of the PVC is blocked (Piper *et al.*, 1995; Babst *et al.*, 1997; Finkeneigen *et al.*, 1997). In contrast to wild-type cells, the PVC in such strains contains substantial vacuolar protease activity. Therefore, the rate of processing of newly synthesized A-ALP in class E mutants such as *vps27*Δ reflects the rate of transport from its site of synthesis at the ER to the PVC. The observed rate of A-ALP processing in the *vps27*Δ *inp53-1* strain (half-time of 25 min) was much faster than in the *vps27*Δ single mutant (50 min), indicating that the step affected by *inp53-1* must be the TGN-to-PVC step or an earlier step (Figure 5A).

Deletion of amino acids 2–11 of the cytoplasmic domain of A-ALP dramatically increases its rate of TGN-to-PVC transport (Bryant and Stevens, 1997), suggesting that this region contains the slow delivery signal or that the 2–11 deletion interferes with the true signal elsewhere in the cytosolic domain. If Inp53p functions in concert with the slow delivery signal, little if any additive effect on the severity of the phenotype would be expected upon combining *inp53* with the Δ2–11 mutation. The A(Δ2–11)-ALP mutant was processed much faster in a *vps27*Δ strain than wild-type A-ALP (Figure 5A; Bryant and Stevens, 1997). Comparison of the rate of processing of A(Δ2–11)-ALP in the *vps27*Δ *inp53-1* strain (16 min, lanes 13–16) to the rates obtained for the A-ALP/*vps27*Δ *inp53-1* and A(Δ2–11)-ALP/*vps27*Δ strains (25 min each; lanes 5–12) indicates that there is some additive effect of the Δ2–11 *cis*-acting and *inp53-1 trans*-acting mutations. These results suggest that Inp53p may act at a different step than that of the 2–11 signal. Alternatively, the two mutations may act at the same step, but the mild additive effect might be due to the fact that one or both of the single mutations may not completely neutralize the slow delivery mechanism.

To test whether Inp53p is required for maintaining slow delivery of Kex2p into the PVC, the rate of Kex2p turnover in *vps27*Δ and *inp53-1 vps27*Δ strains was assessed (Figure 5B). The half-time of Kex2p degradation was shorter in the *inp53-1 vps27*Δ double mutant strain (17 min) than in the *vps27*Δ strain (26 min), indicating that in the absence of Inp53p function Kex2p more rapidly reaches the PVC. The results, taken together with the observation that *inp53-1* exhibited an additive affect with the $Y_{713}A$ mutation in Kex2p, implicate Inp53p function in the slow delivery mechanism for both A-ALP and Kex2p.

The possibility that Inp53p might regulate the rate of ER-to-Golgi transport was assessed by monitoring the rate by which the core *N*-linked oligosaccharide chains of A(F→A)-ALP were extended with α1,6 mannose residues, an event that occurs in an early Golgi compartment (Gaynor *et al.*, 1994). The rate of α1,6 mannose acquisition of A(F→A)-ALP in *inp53-1* strains was indistinguishable from wild type (our unpublished results), suggesting that the early secretory pathway is not affected in the *inp53-1* mutant. Furthermore, the rate of transport of newly synthesized Vps10p to the PVC in class E *vps* cells (see below), and ALP to the vacuole in otherwise wild-type cells (Figure 1C), was

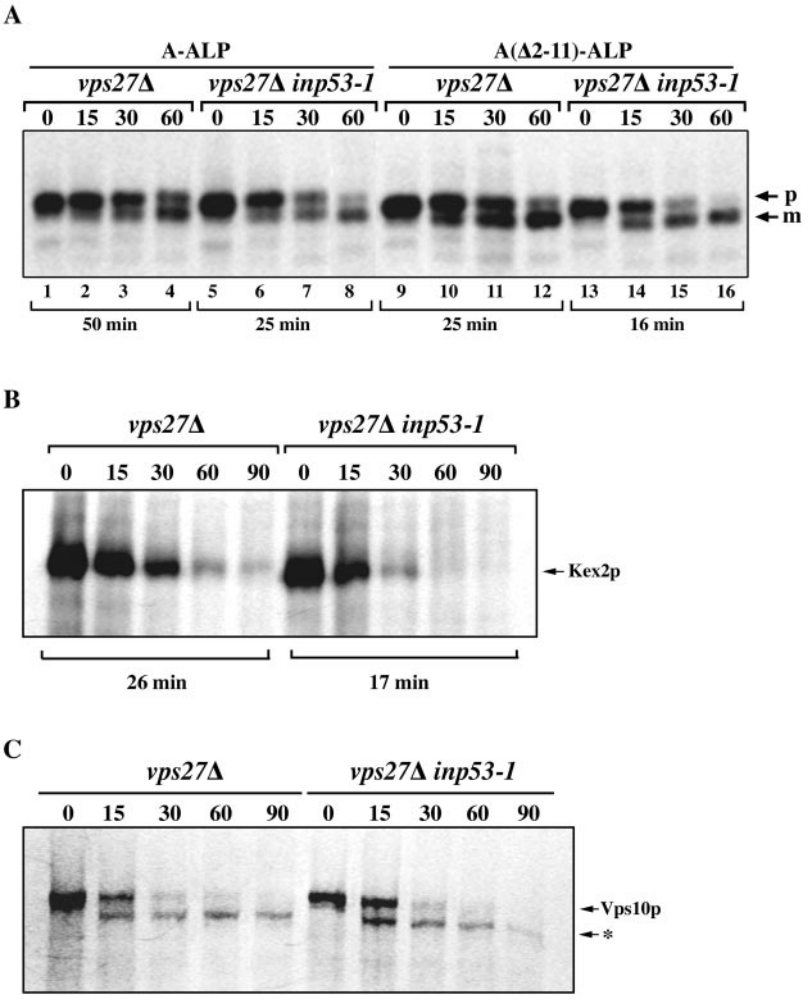

Figure 5. Loss of Inp53p function increases the rate of transport into the PVC of A-ALP and Kex2p but not of Vps10p. In all three panels cells were pulsed with [^{35}S]methionine/cysteine for 10 min before unlabeled amino acids were added to initiate the chase. At the indicated chase times either A-ALP (A), A(Δ2–11)-ALP (A), Kex2p (B), or Vps10p (C) was immunoprecipitated. The following strain plasmid combinations were analyzed in A: SHY42/pAH16, SHY43/pAH16, SHY42/pAH72, and SHY43/pAH72. Strains SHY42 and SHY43 were analyzed in both B and C. Half-times of wild-type or mutant A-ALP, Kex2p, and Vps10p processing/degradation are indicated beneath each panel. Positions of intact Vps10p and a Vps10p breakdown product (*) are indicated in C.

not altered by a loss of Inp53p function. Taken together, the results strongly suggest that Inp53p regulates the rate of TGN-to-PVC transport for A-ALP and Kex2p but does not affect an earlier transport step.

Trafficking of Vps10p Is Normal in inp53 Mutants

In contrast to A-ALP and Kex2p, the CPY-sorting receptor Vps10p is known to undergo rapid transport from the TGN to the PVC (Bryant and Stevens, 1997), suggesting that its transport is not affected by the slow delivery mechanism. Therefore, to test whether the role of Inp53p is specific to the slow delivery mechanism and does not involve other aspects of the TGN-to-PVC transport pathway, we assessed trafficking of Vps10p in *inp53* mutants. We initially analyzed the rate of CPY trafficking and CPY sorting efficiency as a measure of proper localization and trafficking of Vps10p (Figure 6A). Cells were pulsed for 10 min with [^{35}S]methionine/cysteine, chased, and CPY was then immunoprecipitated from the intracellular and extracellular fractions. In the wild-type strain CPY remained intracellular during the time course and was converted from the p1 form (ER) to the p2 form (Golgi), and was finally processed to the mature form (vacuole) as has been previously documented (Stevens *et al.*, 1982). The sorting and rate of trafficking of CPY to the vacuole in *inp53-1* cells were indistinguishable from wild type. Sorting was also unaffected in the *inp53*Δ strain. In contrast, in the *vps35*Δ mutant, known to exhibit defective Vps10p trafficking (Seaman *et al.*, 1997; Nothwehr *et al.*, 1999), most of the CPY is aberrantly secreted.

Vps10p trafficking in wild-type and *inp53* mutant cells was further evaluated by assessing its subcellular localization. Lysates from ^{35}S-labeled cells were centrifuged at 13,000 × *g* to generate supernatant (S13) and pellet (P13) fractions. The S13 fraction was then centrifuged at 150,000 × *g* to generate supernatant (S150) and pellet (P150) fractions. With the use of this type of fractionation scheme (Marcusson *et al.*, 1994; Nothwehr and Hindes, 1997), the P13 contains vacuoles, ER, and plasma membrane, whereas the P150 contains Golgi, endosomes, and vesicles. In wild-type and *inp53-1* cells the majority of Vps10p was found in the P150 fraction (Figure 6B), consistent with a TGN/endosomal localization. Thus, Vps10p localization was not substantially altered due to a loss of Inp53p function.

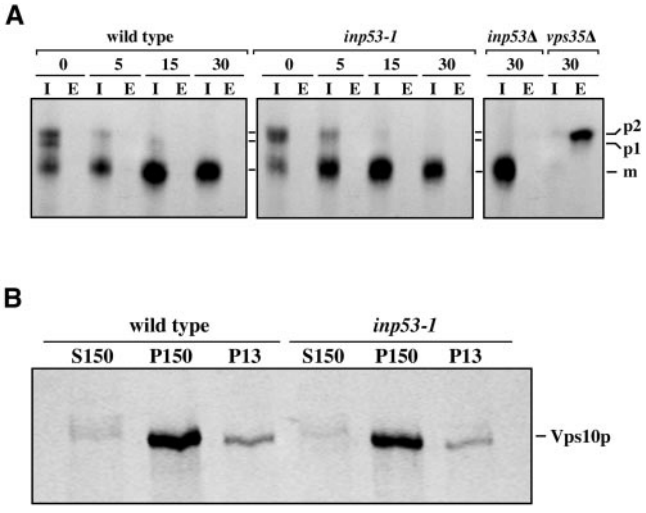

Figure 6. Trafficking and localization of Vps10p are not affected by a loss of Inp53p function. The wild-type, *inp53-1*, *inp53*Δ, and *vps35*Δ strains analyzed were SHY35, SHY40, SHY38, and SNY79, respectively. (A) Strains were pulsed with [^{35}S]methionine/cysteine for 10 min and chased with unlabeled amino acids for 0, 5, 15, and 30 min, or 30 min only, as indicated. CPY was immunoprecipitated from the intracellular (I) and extracellular (E) fractions and analyzed by SDS-PAGE and fluorography. The positions of the ER and Golgi precursor forms of CPY (p1 and p2, respectively), and mature vacuolar form (m), are indicated. (B) Strains were pulsed for 10 min and chased for 60 min. Spheroplasts were then lysed and lysates centrifuged at 13,000 × *g* to generate pellet (P13) and supernatant fractions. The supernatant was then centrifuged at 150,000 × *g* to generate pellet (P150) and supernatant (S150) fractions. Vps10p was immunoprecipitated from each fraction and was analyzed by SDS-PAGE and fluorography.

We next directly examined whether the rate of TGN-to-PVC transport of Vps10p is accelerated in *inp53* mutants as is the case with A-ALP and Kex2p. In class E *vps* mutants Vps10p is proteolytically processed to a faster migrating form upon reaching the exaggerated PVC (Cereghino *et al.*, 1995). We thus analyzed the rate of processing of Vps10p in *vps27*Δ and *vps27*Δ *inp53-1* strains as a measure of its rate of delivery to the PVC (Figure 5C). In contrast to the results for A-ALP and Kex2p (Figure 5, A and B) a loss of Inp53p function caused no change in the rate of delivery of newly synthesized Vps10p to the PVC in *vps27*Δ cells. In addition, a mutant form of Vps10p that fails to be retrieved from the PVC was transported to the vacuole in *inp53-1* cells at the same rate as in wild-type cells (our unpublished results). Taken together, these results suggest that Inp53p is required for maintaining slow delivery of certain resident TGN membrane proteins such as A-ALP into the PVC but does not globally affect the rate of TGN-to-PVC vesicular transport.

inp53-1 Allele Contains a Mutation in Conserved Region of SAC1 Domain

As described above, the *inp53-1* allele exhibited more severe Kex2p mislocalization phenotypes than the *inp53*Δ allele. This finding suggested that mapping the mutation in the *inp53-1* allele might provide insights into structure–function relationships in Inp53p. Sequencing of the *inp53-1* allele revealed that it contained a single G-to-A nucleotide change causing a $G_{473}D$ amino acid change. The G_{473} residue resides in a conserved region of the SAC1 domain just 45 amino acids downstream of a putative conserved catalytic motif, $Cx_5R(T/S)$, common to protein and inositol phosphatases (Figure 7; Guo *et al.*, 1999; Hughes *et al.*, 2000a). Comparison of Inp53p to several related proteins containing SAC1 domains indicates that small aliphatic residues are typically found at this position, with Inp51p representing an exception. However, Inp51p exhibits a significantly lower degree of sequence conservation in the SAC1 domain and has been shown to lack polyphosphoinositide phosphatase activity (Guo *et al.*, 1999). Genetic screening has previously identified six mutant *sac1* alleles that relieve the requirement for *SEC14* and exhibit phenotypes consistent with a loss of phosphatase activity (Kearns *et al.*, 1997). Intriguingly, an $A_{445}V$ mutation was responsible for the phenotype of two of these alleles and the A_{445} residue corresponds to the G_{473} residue of Inp53p (Figure 7). Thus, the SAC1 domain of the *inp53-1* gene product is most likely defective, whereas the 5-phosphatase domain may retain function as suggested by the interfering function exhibited by the *inp53-1* gene product.

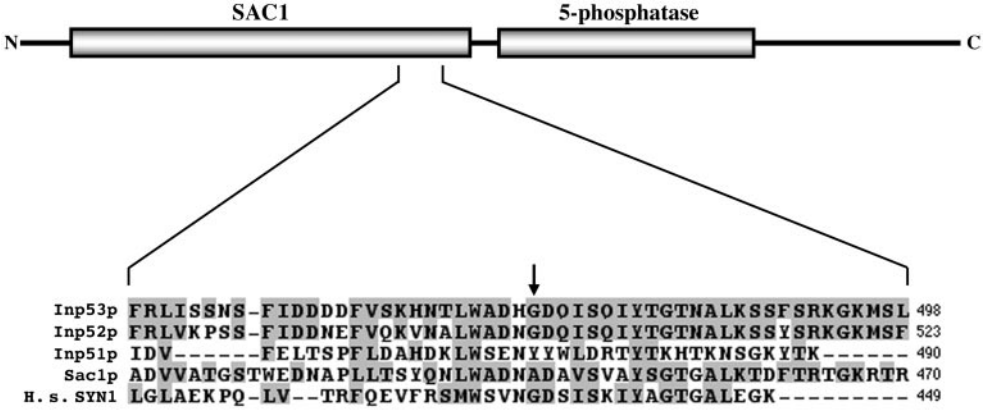

Figure 7. Inp53p contains two separate phosphoinositide phosphatase domains. Sequence comparisons among *S. cerevisiae* Inp53p, *S. cerevisiae* Inp52p, *S. cerevisiae* Inp51p, *S. cerevisiae* *Sac*Ip, and *Homo sapiens* synaptojanin were performed with the use of the MAP program (Huang, 1994). Regions exhibiting extensive amino acid conservation are shaded. The Gly_{473} residue in Inp53p that was mutated to Asp in the protein encoded by the *inp53-1* allele is indicated (arrow). The entire sequences were used in the alignment, although only the region in the vicinity of Gly_{473} residue of Inp53p is shown. The SAC1 domain and 5-phosphatase regions were assigned to residues 60–530 and 564–864, respectively.

Strains Containing Mutations in INP53 Exhibit Little or No Detectable Changes in Phosphoinositide Levels

The defects observed in trafficking and localization of A-ALP and Kex2p in *inp53* mutant strains were probably due to a lack of polyphosphoinositide phosphatase activity (Guo *et al.*, 1999). Therefore, the distinct phenotypic behavior of the *inp53*Δ, *inp53-1* and wild-type strains might be reflected in differences in phosphoinositide levels in these strains. A previous report indicated that an *inp53* null mutant strain did not exhibit changes in the level of PtdIns(4,5)P_2 compared with wild type as analyzed by thin layer chromatography (Stolz *et al.*, 1998), but it was not known whether other phosphoinositide species were affected. We thus used HPLC to analyze the in vivo levels of the four phosphoinositides, PtdIns(3)P, PtdIns(4)P, PtdIns(3,5)P_2, and PtdIns(4,5)P_2, in total cell extracts from wild-type, *inp53-1*, and *inp53*Δ strains. Only a very subtle increase in the level of all four phosphoinositide species was observed in the *inp53*Δ and *inp53-1* mutants compared with wild type and no differences could be discerned between the mutants (Figure 8).

Portion of Inp53p Associates with Slowly Sedimenting Membrane Fraction

The finding that Inp53p regulated the rate of TGN-to-PVC transport suggested that it associated with the periphery of the TGN or an endosomal compartment. To test this idea, specific antisera were raised against Inp53p and cell fractionation experiments were performed with the use of a similar approach as described in the legend to Figure 6B. P15, P200, and S200 fractions were analyzed by Western blot detection of vacuolar (Vph1p), TGN (Kex2p), and soluble (phosphoglycerol kinase) protein markers in addition to Inp53p (Figure 9). As expected, the majority of Vph1p and Kex2p fractionated in the P15 and P200 fractions, respectively, whereas phosphoglycerol kinase remained in the soluble (S200) fraction. Most of the Inp53p fractionated with soluble proteins in the S200 fraction consistent with the lack of predicted transmembrane domain sequences found in analyses of the Inp53p sequence. However, we consistently observed ~20–25% of Inp53p sedimenting in the P200 pellet. Little or no Inp53p was found in the P15 pellet. Taken together, these results suggest that Inp53p associates as a peripheral membrane protein with Golgi, endosomal, or vesicular membranes.

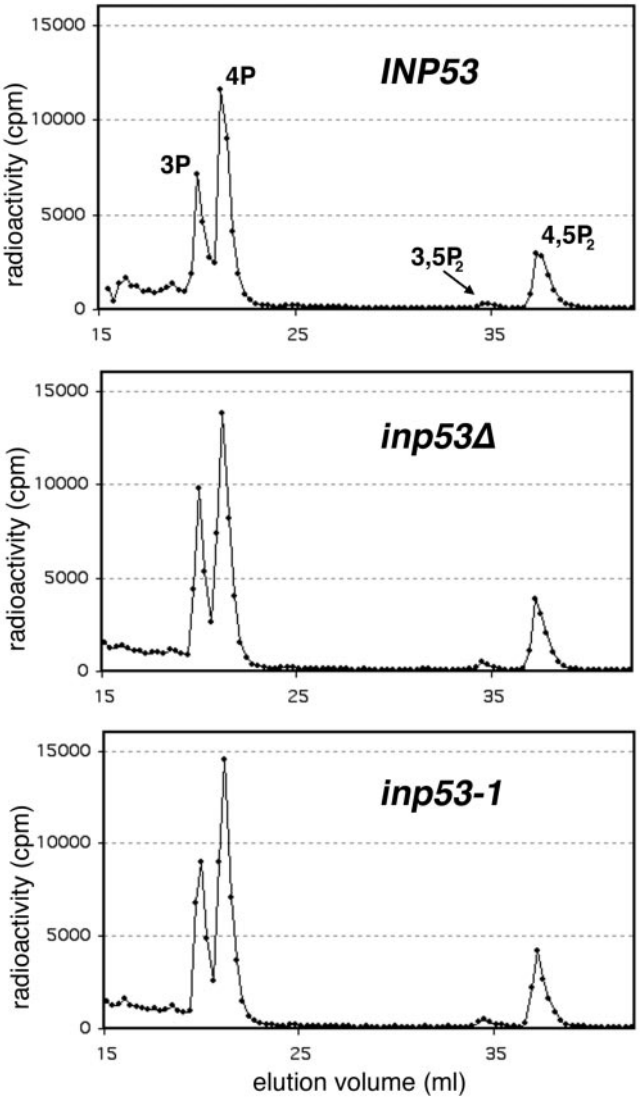

Figure 8. Phosphoinositide levels are similar in wild-type and *inp53* mutant cells. Strains SHY35 (*INP53*), SHY38 (*inp53*Δ), and SHY40 (*inp53-1*) were metabolically labeled with [^{3}H]myo-inositiol at 30°C. Cellular lipids were extracted, deacylated, and the resulting glycerophosphoinositols were resolved with the use of ion-exchange HPLC. The elution positions of glycerophosphoinositol 3-phosphate (3P), glycerophosphoinositol 4-phosphate (4P), glycerophosphoinositol3,5-bisphosphate(3,5P_2),andglycerophosphoinositol 4,5-bisphosphate (4,5P_2) are indicated.

DISCUSSION

This study is the first to identify and characterize a component of the machinery responsible for maintaining a slow rate of TGN-to-PVC transport for TGN resident proteins. A genetic strategy led to identification of a novel mutant allele of the *INP53* gene that encodes an inositol polyphosphate 5-phosphatase. Phenotypic characterization of this allele, *inp53-1*, and the null allele *inp53*Δ indicated that a loss of Inp53p function accelerated the rate of vacuolar transport of A(F→A)-ALP, a retrieval-defective TGN protein. Further analysis demonstrated that this increase in transport rate was due to accelerated TGN-to-PVC transport and that both A-ALP and Kex2p were affected. This defect was highly specific because the rate of TGN-to-PVC trafficking of Vps10p was unaffected. The phenotypic effect of combining mutations in *INP53* with mutations that block retrieval from the PVC strongly suggests that Inp53p plays no role in the retrieval process. A loss of Inp53p function also had no effect on the AP-3–dependent transport of ALP to the vacuole. Thus, a loss of Inp53p function does not appear to cause general defects in TGN function but rather affects regulation in TGN-to-PVC transport for certain cargo molecules. The role of Inp53p in phospholipid metabolism (Srinivasan *et al.*, 1997; Stolz *et al.*, 1998) argues that a critical balance in the

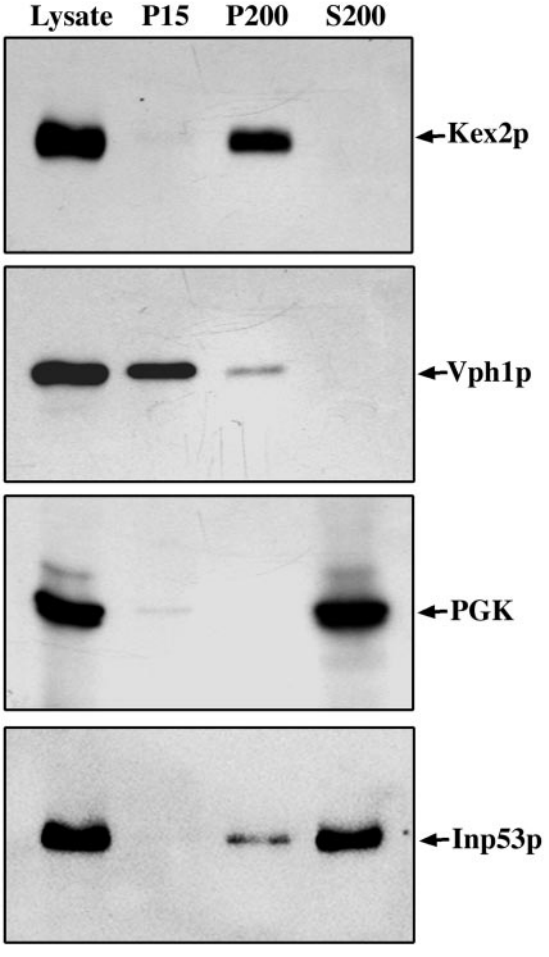

Figure 9. Inp53p exhibits both a soluble and a membrane-associated pool that sediments at high speed. Strain SEY6210 was spheroplasted, lysed in hypotonic buffer, and subjected to centrifugation at 15,000 × *g* to generate pellet (P15) and supernatant fractions. The supernatant was then centrifuged at 200,000 × *g* to generate pellet (P200) and supernatant (S200) fractions. Fractions were resolved by SDS-PAGE and immunoblotted with the use of antibodies against Kex2p, Vph1p, phosphoglycerol kinase (PGK), and Inp53p.

level of one or more phosphoinositides is necessary for proper regulation of trafficking of TGN residents A-ALP and Kex2p.

Inp53p is a member of the synaptojanin family of proteins that is involved in a diverse set of processes. For example, synaptojanin itself is known to be required for multiple steps in synaptic vesicle recycling, including budding of vesicles from the plasma membrane, uncoating of vesicles after fission, tethering of vesicles to the cytoskeleton, and recycling of vesicles back to the plasma membrane (Cremona *et al.*, 1999; Harris *et al.*, 2000). The three yeast genes that most closely resemble mammalian synaptojanin, *INP51*, *INP52*, and *INP53*, have been previously analyzed for phenotypes in membrane-trafficking events, organelle dynamics, and actin cytoskeletal regulation. Analysis of strains containing individual disruptions of the three genes resulted in little or no defect in growth, vacuolar morphology, vacuolar protein sorting, or endocytic uptake of the lipophilic dye FM4-64 (Srinivasan *et al.*, 1997; Singer-Krüger *et al.*, 1998; Stolz *et al.*, 1998). The lack of a vacuolar protein-sorting defect is in agreement with our observation that localization and trafficking of the CPY receptor Vps10p is normal in *inp53*Δ and *inp53-1* strains. Various double mutant combinations also exhibited no vacuolar protein sorting or secretion defects but resulted in varying levels of endocytic pathway defects. For example, an *inp51 inp52* combination exhibited marked endocytic defects, *inp52 inp53* was less severe, and *inp51 inp53* behaved like wild type (Singer-Krüger *et al.*, 1998). Similarly, *inp51 inp52* and *inp52 inp53* strains exhibited a slow growth phenotype and a defect in actin polarization but an *inp51 inp53* strain did not (Srinivasan *et al.*, 1997; Stolz *et al.*, 1998). Taken together, these observations suggest that the Inp proteins have some overlapping functions but unique roles as well. We observed no trafficking defect in the AP-3–dependent vacuolar trafficking pathway in an *inp53* mutant; however, it is possible that Inp53p function might be redundant with another phosphoinositide phosphatase for this specific process.

The 5-phosphatase domain of Inp53p has been shown in vitro to hydrolyze the C5 phosphate moiety from PtdIns(4,5)P_2 to generate PtdIns(4)P but does not use PtdIns(3,5)P_2, PtdIns(3)P, or PtdIns(4)P as a substrate (Guo *et al.*, 1999). In contrast, the SAC1 domain dephosphorylates PtdIns(3,5)P_2, PtdIns(3)P, and PtdIns(4)P to PtdIns but does not act on PtdIns(4,5)P_2. Among the three Inp proteins, Inp53p has been shown to contribute the most PtdIns(4,5)P_2 dephosphorylating activity (Srinivasan *et al.*, 1997). However, we observed little or no difference in in vivo PtdIns(3)P, PtdIns(4)P, PtdIns(3,5)P_2, or PtdIns(4,5)P_2 levels in *inp53* mutants compared with wild type. These results are in accordance with the lack of global phenotypic defects in *inp53* mutants such as cell growth, endocytosis, and cell wall defects. The highly specific defect we have observed in trafficking between the TGN and PVC is probably due to a localized change in the level of one or more phosphoinositides at a specific membrane domain in the cell. Precedence for this idea comes from the fact that PtdIns(3,5)P_2 is present in barely detectable levels in phosphoinositide analyses yet its synthesis at the PVC membrane triggers protein sorting into the multivesicular body pathway (Odorizzi *et al.*, 1998). Analysis of phosphoinositide levels in specific intracellular compartments in *inp53* mutants will be needed to address the connection between phosphoinositide levels and regulation of TGN-to-PVC trafficking.

Clues regarding the roles of phosphoinositides in membrane traffic have recently emerged. The levels of phosphoinositide species are modulated by both lipid kinases and phosphatases. Effector proteins that bind to PtdIns(3)P via a FYVE domain and are involved in membrane fusion have been identified in both yeast and mammals (Stenmark *et al.*, 1996; Burd and Emr, 1998; Simonsen *et al.*, 1998). Effector proteins that bind to PtdIns(4,5)P_2 via an ENTH domain and are involved in recruiting clathrin-mediated endocytic machinery have also been identified (Ford *et al.*, 2001; Itoh *et al.*, 2001). Phosphoinositide phosphatases such as Inp53p are thought to dampen or terminate phosphoinositide signaling pathways. This could occur by removal of the phosphoinositide that acts as a binding site for an effector, thereby leading to dissociation of the effector protein from the mem-

brane. Such clearing of effector proteins from the membrane after they have performed their function would make them available for another iteration of their function, e.g., facilitating vesicle formation.

An unexpected finding in this work was the more severe phenotypes observed for the *inp53-1* mutant compared with the *inp53*Δ mutant. The *inp53-1* allele is recessive and thus the mutant protein expressed from this allele does not interfere in any obvious way when the wild-type protein is present. One possibility is that in the absence of wild-type Inp53p, a mechanism compensates to reduce the extent of the defect, however; the protein expressed from *inp53-1* interferes with this compensating mechanism. The *inp53-1* allele contains a $G_{473}D$ mutation within the SAC1 domain. The fact that an analogous mutation inactivates Saclp itself (Kearns *et al.*, 1997) suggests that the protein encoded by *inp53-1* may have lost the ability to dephosphorylate PtdIns(3,5)P_2, PtdIns(3)P, and PtdIns(4)P but has retained the ability to act on PtdIns(4,5)P_2 because its 5-phosphatase domain would still be intact. Testing of this idea awaits the in vitro analysis of enzyme activity of the *inp53-1* gene product.

Surprisingly, the difference in phenotypes between the *inp53-1* and *inp53*Δ alleles was observed for Kex2p trafficking but not for A-ALP. Additionally, the localization defects caused by mutations in *INP53* were only apparent in the retrieval-defective form of A-ALP, whereas both wild-type and retrieval-defective forms of Kex2p were substantially affected. Even in wild-type strains Kex2p exhibits more rapid vacuolar degradation than does A-ALP, suggesting some aspect of its localization mechanism is not as efficient as that of A-ALP (Wilcox *et al.*, 1992; Nothwehr *et al.*, 1993). It is possible that retrieval from the PVC is more efficient for A-ALP than for Kex2p and, as a result, Kex2p relies more heavily on the slow delivery mechanism than does A-ALP.

How might Inp53p affect the rate of TGN-to-PVC traffic of certain types of membrane protein cargo? The basis of the mechanism for maintaining a slow rate of transport between the TGN and PVC for TGN resident proteins is not well understood. On discovery of localization signals in the cytosolic domains of Kex2p and DPAP A (A-ALP) that were distinct from the PVC retrieval signals, it was assumed that these signals would simply prevent rapid exit from the TGN, and the loss of such signals would permit rapid TGN-to-PVC transport (Brickner and Fuller, 1997; Bryant and Stevens, 1997). Such static retention models assume that the TGN is a stable compartment. According to this view (Figure 10A), Inp53p may act at the TGN to negatively regulate entry of A-ALP and Kex2p into TGN-derived vesicles that fuse with the PVC. In the absence of Inp53p function A-ALP and Kex2p enter such vesicles more frequently, reflecting an increased rate of TGN-to-PVC transport.

However, recent data on A-ALP and Kex2p trafficking suggest a more complex trafficking itinerary than previously thought. Rather than being a stable compartment, new evidence suggests that the TGN may form by directed maturation from earlier Golgi compartments and that TGN compartments would eventually mature into vesicles and post-TGN compartments (Glick *et al.*, 1997; Bonfanti *et al.*, 1998; Mironov *et al.*, 1998; Allan and Balch, 1999). There is good morphological and functional evidence for the existence of an early endosomal compartment that is distinct from the late endosome/PVC (Singer-Krüger *et al.*, 1993; Prescianotto-Baschong and Riezman, 1998; Lewis *et al.*, 2000). Recycling of the late secretory v-SNARE Snc1p appears to involve transport from the plasma membrane to an early endosomal compartment. Snc1p then is transported to the TGN, a step dependent upon a sorting signal in Snc1p (Lewis *et al.*, 2000). As proposed by Pelham and coworkers, the existence of an early endosome-to-TGN pathway suggests that resident TGN membrane proteins may also use this pathway in addition to the PVC-to-TGN pathway. Accordingly, the signals on A-ALP and Kex2p that slow delivery to the PVC might actually be early endosome retrieval signals. Loss of these signals would cause transport from the early endosome to the PVC by default where A-ALP and Kex2p could be retrieved via the retromer back to the TGN. Thus, in the absence of the slow delivery signal, a TGN protein would visit the PVC much more frequently reflecting an increased overall rate of TGN-to-PVC transport. This model would predict that Vps10p cycling is restricted to a more direct TGN-to-PVC route, which makes sense given its role in CPY sorting. Interestingly, the existence of two pathways for exit from the yeast TGN to endosomes has recently been proposed: a selective one mediated by the GGA coat proteins and a nonselective one (Black and Pelham, 2000).

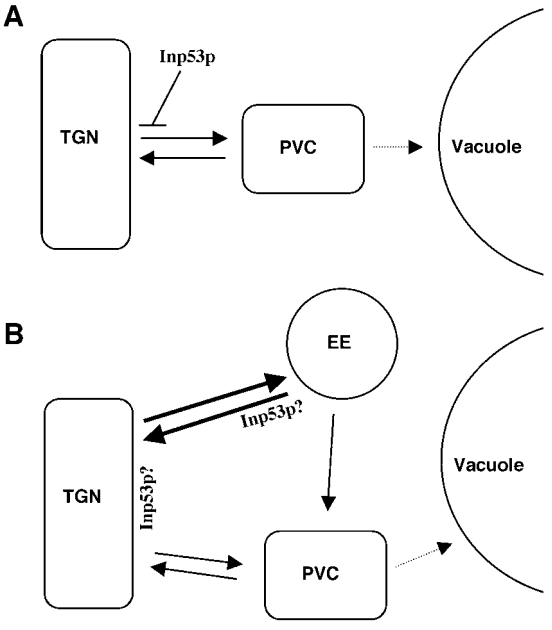

Figure 10. Models for the point of execution of Inp53p function in TGN protein localization. (A) Inp53p function is considered in the context of a model in which the TGN is a stable compartment and resident TGN proteins only cycle between the TGN and the PVC. The horizontal bar represents inhibition of TGN-to-PVC transport. (B) Inp53p function considered in the context of a model in which the TGN undergoes directed maturation. In this model TGN resident proteins frequently cycle to and from an early endosomal organelle (EE). The extent to which a pathway is used by TGN resident proteins is proportional to the thickness of the arrow representing the pathway. See text for details.

Assuming that TGN resident proteins such as A-ALP frequently cycle between the TGN and an early endosomal compartment and less frequently cycle between the TGN and PVC, two basic models for Inp53p function can be proposed (Figure 10B). In the first model, Inp53p functions at the TGN where it positively regulates entry of A-ALP into vesicles for delivery to the early endosome. A loss of Inp53p function causes A-ALP to exclusively enter TGN-derived vesicles for direct delivery to the PVC. These same vesicles may also carry Vps10p:CPY complexes. Alternatively, Inp53p could negatively regulate entry into the direct TGN-to-PVC pathway and thus allow A-ALP to use the TGN-to-early endosome pathway by default. A second model proposes that Inp53p localizes to the early endosome where it is required for retrieval of A-ALP back to the TGN (Figure 10B). In the absence of Inp53p function, TGN residents at the early endosome would be shunted to the PVC by default rather than being retrieved to the TGN. At the PVC, A-ALP could be retrieved back to the TGN. In accordance with our observed data, both of the models predict that defects in the slow delivery mechanism would not affect Vps10p trafficking because Vps10p exclusively reaches the PVC via a direct route from the TGN.

Analysis of Inp53p subcellular localization is consistent with a role in regulating membrane traffic between the TGN and endosomes. Although the majority of Inp53p fractionated with the soluble, cytosolic fraction, a smaller pool was associated with a high-speed (200,000 $\times$ *g*) particulate fraction containing the TGN marker Kex2p. Little or no Inp53p sedimented at 15,000 $\times$ *g*. These results contrast with a previous study (Stolz *et al.*, 1998) reporting that most of Inp53p pelleted from a cell lysate at 20,000 $\times$ *g*. However, the fractionation of a cytosolic control protein was not reported; thus, it is possible that the results of this previous study could be explained by inefficient cell lysis. Our efforts to localize Inp53p by immunofluorescence microscopy have been unsuccessful to date. However, Inp52p and Inp53p tagged with green fluorescent protein have recently been visualized in yeast when overproduced (Ooms *et al.*, 2000). These proteins predominantly exhibit a diffuse cytoplasmic staining pattern consistent with our biochemical fractionation results. However, when cells are placed under osmotic stress both tagged proteins rapidly colocalized with actin cortical patches on the plasma membrane. It is thought that under osmotic stress conditions Inp52p and Inp53p may play a role regulating actin polymerization and assembly. We observed little if any Inp53p in the P15 fraction, the expected destination of plasma membranes, suggesting that in nonstressed cells Inp53p does not associate with the plasma membrane. Taken together, these data are consistent with the idea that Inp53p cycles between soluble and membrane-associated states and that it has multiple membrane targets.

The models illustrated in Figure 10 predict that Inp53p is involved in vesicle formation or in regulating the entry of TGN resident protein cargo into budding vesicles at either the TGN or early endosome. This idea fits well with recent work suggesting a role for Inp53p in membrane trafficking in the TGN/endosomal system. A mutant form of the plasma membrane ATPase Pma1p, that is normally shunted to the vacuole rather than its normal destination, was used to identify yeast mutants that deliver the Pma1p mutant to the plasma membrane (Luo and Chang, 1997). In addition to genes required for normal vacuolar biogenesis, PVC-to-vacuole traffic, and trafficking between the TGN and PVC, the screen identified *INP53*. These data imply that A(F→A)-ALP might also be initially transported to plasma membrane in *inp53-1* cells before reaching the PVC and vacuole via the endocytic pathway. However, this does not appear to be the case because A(F→A)-ALP reaches the vacuole in *inp53-1* cells in an End3p-independent manner (Ha and Nothwehr, unpublished results). Mutations in *INP53* have also been shown to exhibit synthetic growth and pro-α-factor secretion phenotypes when combined with a clathrin heavy chain temperature-sensitive mutant (Bensen *et al.*, 2000). These studies suggest that Inp53p may participate in clathrin-mediated sorting at the TGN, and fit well with our finding that regulation of TGN-to-endosome traffic is altered in *inp53* mutants. Future studies aimed at identifying the site of Inp53p action and its downstream effectors will aid in understanding the mechanism for maintaining a slow rate of TGN protein delivery to the PVC.

ACKNOWLEDGMENTS

We acknowledge Scott Emr, Tom Stevens, and Greg Payne for the generous contribution of antibodies. David Eide provided valuable critical evaluation of the manuscript. This work was supported by grants from the National Institutes of Health (GM-53449) and American Cancer Society awarded to S.F.N. and D.B.D., respectively.

REFERENCES

Allan, R.B., and Balch, W.E. (1999). Protein sorting by directed maturation of Golgi compartments. Science *285*, 63–66.

Babst, M., Sato, T.K., Banta, L.M., and Emr, S.D. (1997). Endosomal transport function in yeast requires a novel AAA-type ATPase, Vps4p. EMBO J. *16*, 1820–1831.

Bensen, E.S., Costaguta, G., and Payne, G.S. (2000). Synthetic genetic interactions with temperature-sensitive clathrin *Saccharomyces cerevisiae*: roles for synaptojanin-like Inp53p and dynamin-related Vps1p in clathrin-dependent protein sorting at the trans-Golgi network. Genetics *154*, 83–97.

Bensen, E.S., Yeung, B.G., and Payne, G.S. (2001). Ric1p and the Ypt6p GTPase function in a common pathway required for localization of *trans*-Golgi network membrane proteins. Mol. Biol. Cell *12*, 13–26.

Black, M.W., and Pelham, H.R.B. (2000). A selective transport route from Golgi to late endosomes that requires the yeast GGA proteins. J. Cell Biol. *151*, 587–600.

Bonfanti, L., Mironov, A.A.J., Martinex-Menarguez, J.A., Martella, O., Fusella, A., Baldassarre, M., Buccione, R., Geuze, H.J., Mironov, A.A., and Luini, A. (1998). Procollagen traverses the Golgi stack without leaving the lumen of cisternae: evidence for cisternal maturation. Cell *95*, 993–1003.

Brickner, J.H., and Fuller, R.S. (1997). *SOI1* encodes a novel, conserved protein that promotes TGN-endosomal cycling of Kex2p and other membrane proteins by modulating the function of two TGN localization signals. J. Cell Biol. *139*, 23–26.

Bryant, N.J., and Stevens, T.H. (1997). Two separate signals act independently to localize a yeast late Golgi membrane protein through a combination of retrieval and retention. J. Cell Biol. *136*, 287–297.

Burd, C.G., and Emr, S.D. (1998). Phosphatidylinositol(3)-phosphate signaling mediated by specific binding to ring FYVE domains. Mol. Cell *2*, 157–162.

Cereghino, J.L., Marcusson, E.G., and Emr, S.D. (1995). The cytoplasmic tail domain of the vacuolar protein sorting receptor Vps10p and a subset of *VPS* gene products regulate receptor stability, function, and localization. Mol. Biol. Cell *6*, 1089–1102.

Chapman, R., and Munro, S. (1994). The functioning of the yeast Golgi apparatus requires an ER protein encoded by *ANP1*, a member of a new family of genes affecting the secretory pathway. EMBO J. *13*, 4896–4907.

Cooper, A., and Bussey, H. (1992). Yeast Kex1p is a Golgi-associated membrane protein: deletions in a cytoplasmic targeting domain result in mislocalization to the vacuolar membrane. J. Cell Biol. *119*, 1459–1468.

Cooper, A.A., and Stevens, T.H. (1996). Vps10p cycles between the late-Golgi and prevacuolar compartments in its function as the sorting receptor for multiple yeast vacuolar hydrolases. J. Cell Biol. *133*, 529–541.

Cowles, C.R., Odorizzi, G., Payne, G.S., and Emr, S.D. (1997a). The AP-3 adaptor complex is essential for cargo-selective transport to the yeast vacuole. Cell *91*, 109–118.

Cowles, C.R., Snyder, W.B., Burd, C.G., and Emr, S.D. (1997b). Novel Golgi to vacuole delivery pathway in yeast—identification of a sorting determinant and required transport component. EMBO J. *16*, 2769–2782.

Cremona, O., Di Paolo, G., Wenk, M.R., Luthi, A., Kim, W.T., Takei, K., Daniell, L., Nemoto, Y., Shears, S.B., Flavell, R.A., McCormick, D.A., and De Camilli, P. (1999). Essential role of phosphoinositide metabolism in synaptic vesicle recycling. Cell *99*, 179–188.

Finkeneigen, M., Rohricht, R.A., and Kohrer, K. (1997). The *VPS4* gene is involved in protein transport out of a yeast prevacuolar endosome-like compartment. Curr. Genet. *31*, 469–480.

Ford, M.G.J., Pearse, B.M.F., Higgins, M.K., Vallis, Y., Owen, D.J., Gibson, D., Hopkins, C.R., Evans, P.R., and McMahon, H.T. (2001). Simultaneous binding of PtdIns(4,5)P_2 and clathrin by AP180 in the nucleation of clathrin lattices on membranes. Science *291*, 1051–1055.

Fuller, R.S., Brake, A.J., and Thorner, J. (1989). Intracellular targeting and structural conservation of a prohormone-processing endoprotease. Science *246*, 482–486.

Fuller, R.S., Sterne, R.E., and Thorner, J. (1988). Enzymes required for yeast prohormone processing. Annu. Rev. Physiol. *50*, 345–362.

Gaynor, E.C., S. te Heesen, T.R. Graham, M. Aebi, and S.D. Emr. (1994). Signal-mediated retrieval of a membrane protein from the Golgi to the ER in yeast. J. Cell Biol. *127*, 653–665.

Glick, B.S., Elston, T., and Oster, G. (1997). A cisternal maturation mechanism can explain the asymmetry of the Golgi stack. FEBS Lett. *414*, 177–181.

Guo, S.L., Stolz, L.E., Lemrow, S.M., and York, J.D. (1999). SAC1-like domains of yeast SAC1, INP52, and INP53 and of human synaptojanin encode polyphosphoinositide phosphatases. J. Biol. Chem. *274*, 12990–12995.

Hama, H., Takemoto, J.Y., and DeWald, D.B. (2000). Analysis of phosphoinositides in protein trafficking. Methods. *20*, 465–473.

Hanson, B.A., and Lester, R.L. (1980). The extraction of inositol-containing phospholipids and phosphatidylcholine from *Saccharomyces cerevisiae* and *Neurospora crassa*. J. Lipid Res. *21*, 309–315.

Harris, T.W., Hartwieg, E., Horvitz, R.H., and Jorgensen, E.M. (2000). Mutations in synaptojanin disrupt synaptic vesicle recycling. J. Cell Biol. *150*, 589–599.

Horazdovsky, B.F., Davies, B.A., Seaman, M.N.J., McLaughlin, S.A., Yoon, S., and Emr, S.D. (1997). A sorting nexin-1 homologue, Vps5p, forms a complex with Vps17p and is required for recycling the vacuolar protein-sorting receptor. Mol. Biol. Cell *8*, 1529–1541.

Huang, X. (1994). On global sequence alignment. Comput. Appl. Biosci. *10*, 227–235.

Hughes, W.E., Cooke, F.T., and Parker, P.J. (2000a). Sac phosphatase domain proteins. Biochem. J. *350*, 337–352.

Hughes, W.E., Woscholski, R., Cooke, F.T., Patrick, R.S., Dove, S.K., McDonald, N.Q., and Parker, P.J. (2000b). SAC1 encodes a regulated lipid phosphoinositide phosphatase, defects in which can be suppressed by the homologous Inp52p and Inp53p phosphatases. J. Biol. Chem. *275*, 801–808.

Itoh, T., Koshiba, S., Kigawa, T., Kikuchi, A., Yokoyama, S., and Takenawa, T. (2001). Role of the ENTH domain in phosphatidylinositol-4,5-bisphosphate binding and endocytosis. Science *291*, 1047–1051.

Kearns, B.G., McGee, T.P., Mayinger, P., Gedvilaite, A., Phillips, S.E., Kagiwada, S., and Bankaitis, V.A. (1997). Essential role for diacylglycerol in protein transport from the yeast Golgi complex. Nature *387*, 101–105.

Lewis, M.J., Nichols, B.J., Prescianotto-Baschong, C., Riezman, H., and Pelham, H.R.B. (2000). Specific retrieval of the exocytic SNARE Snc1p from early yeast endosomes. Mol. Biol. Cell *11*, 23–38.

Luo, W.J., and Chang, A. (1997). Novel genes involved in endosomal traffic in yeast revealed by suppression of a targeting-defective plasma membrane ATPase mutant. J. Cell Biol. *138*, 731–746.

Marcusson, E.G., Horazdovsky, B.F., Cereghino, J.L., Gharakhanian, E., and Emr, S.D. (1994). The sorting receptor for yeast vacuolar carboxypeptidase Y is encoded by the *VPS10* gene. Cell *77*, 579–586.

Mironov, A., Luini, A., and Mironov, A. (1998). A synthetic model of intra-Golgi traffic. FASEB J. *12*, 249–252.

Nothwehr, S.F., Bruinsma, P., and Strawn, L.S. (1999). Distinct domains within Vps35p mediate the retrieval of two different cargo proteins from the yeast prevacuolar/endosomal compartment. Mol. Biol. Cell *10*, 875–890.

Nothwehr, S.F., Bryant, N.J., and Stevens, T.H. (1996). The newly identified yeast *GRD* genes are required for retention of late-Golgi membrane proteins. Mol. Cell. Biol. *16*, 2700–2707.

Nothwehr, S.F., Conibear, E., and Stevens, T.H. (1995). Golgi and vacuolar membrane proteins reach the vacuole in *vps1* mutant yeast cells via the plasma membrane. J. Cell Biol. *129*, 35–46.

Nothwehr, S.F., Ha, S.-A., and Bruinsma, P. (2000). Sorting of yeast membrane proteins into an endosome-to-Golgi pathway involves direct interaction of their cytosolic domains with Vps35p. J. Cell Biol. *151*, 297–309.

Nothwehr, S.F., and Hindes, A.E. (1997). The yeast *VPS5/GRD2* gene encodes a sorting nexin-1-like protein required for localizing membrane proteins to the late Golgi. J. Cell Sci. *110*, 1063–1072.

Nothwehr, S.F., Roberts, C.J., and Stevens, T.H. (1993). Membrane protein retention in the yeast Golgi apparatus: dipeptidyl aminopeptidase A is retained by a cytoplasmic signal containing aromatic residues. J. Cell Biol. *121*, 1197–1209.

Odorizzi, G., Babst, M., and Emr, S.D. (1998). Fab1p PtdIns(3)P 5-kinase function essential for protein sorting in the multivesicular body. Cell *95*, 847–858.

Ooms, L.M., McColl, B.K., Wiradjaja, F., Wijayaratnam, A.P.W., Gleeson, P., Gething, M.J., Sambrook, J., and Mitchell, C.A. (2000). The yeast inositol polyphosphate 5-phosphatases Inp52p and Inp53p translocate to actin patches following hyperosmotic stress: mechanism for regulating phosphatidylinositol 4,5-bisphosphate at plasma membrane invaginations. Mol. Cell. Biol. *20*, 9376–9390.

Orr-Weaver, T.L., Szostak, J.W., and Rothstein, R.J. (1983). Genetic applications of yeast transformation with linear and gapped plasmids. Methods Enzymol. *101*, 228–245.

Piper, R.C., Bryant, N.J., and Stevens, T.H. (1997). The membrane protein alkaline phosphatase is delivered to the vacuole by a route that is distinct from the *vps*-dependent pathway. J. Cell Biol. *138*, 531–545.

Piper, R.C., Cooper, A.A., Yang, H., and Stevens, T.H. (1995). *VPS27* controls vacuolar and endocytic traffic through a prevacuolar compartment in *Saccharomyces cerevisiae*. J. Cell Biol. *131*, 603–617.

Prescianotto-Baschong, C., and Riezman, H. (1998). Morphology of the yeast endocytic pathway. Mol. Biol. Cell *9*, 173–189.

Raymond, C.K., Howald-Stevenson, I., Vater, C.A., and Stevens, T.H. (1992). Morphological classification of the yeast vacuolar protein sorting mutants: evidence for a prevacuolar compartment in class E *vps* mutants. Mol. Biol. Cell *3*, 1389–1402.

Redding, K., Holcomb, C., and Fuller, R.S. (1991). Immunolocalization of Kex2 protease identifies a putative late Golgi compartment in the yeast *Saccharomyces cerevisiae*. J. Cell Biol. *113*, 527–538.

Roberts, C.J., Nothwehr, S.F., and Stevens, T.H. (1992). Membrane protein sorting in the yeast secretory pathway: evidence that the vacuole may be the default compartment. J. Cell Biol. *119*, 69–83.

Roberts, C.J., Raymond, C.K., Yamashiro, C.T., and Stevens, T.H. (1991). Methods for studying the yeast vacuole. Methods Enzymol. *194*, 644–661.

Robinson, J.S., Klionsky, D.J., Banta, L.M., and Emr, S.D. (1988). Protein sorting in *Saccharomyces cerevisiae*: isolation of mutants defective in the delivery and processing of multiple vacuolar hydrolases. Mol. Cell. Biol. *8*, 4936–4948.

Rose, M.D., Novick, P., Thomas, J.H., Botstein, D., and Fink, G.R. (1987). A *Saccharomyces cerevisiae* genomic plasmid bank based on a centromere-containing shuttle vector. Gene *60*, 237–243.

Seaman, M.N.J., Marcusson, E.G., Cereghino, J.L., and Emr, S.D. (1997). Endosome to Golgi retrieval of the vacuolar protein sorting receptor, Vps10p, requires the function of the Vps29, Vps30, and Vps35 gene products. J. Cell Biol. *137*, 79–92.

Seaman, M.N.J., McCaffery, J.M., and Emr, S.D. (1998). A membrane coat complex essential for endosome-to-Golgi retrograde transport in yeast. J. Cell Biol. *142*, 665–681.

Serunian, L.A., Auger, K.R., and Cantley, L.C. (1991). Identification and quantification of polyphosphoinositides produced in response to platelet-derived growth factor stimulation. Methods Enzymol. *198*, 78–87.

Sikorski, R.S., and Hieter, P. (1989). A system of shuttle vectors and yeast host strains designed for efficient manipulation of DNA in *Saccharomyces cerevisiae*. Genetics *122*, 19–27.

Simonsen, A., Lippe, R., Christoforidis, S., Gaullier, J.M., Brech, A., Callaghan, J., Toh, B.H., Murphy, C., Zerial, M., and Stenmark, H. (1998). EEA1 links PI(3)kinase function to rab5 regulation of endosome fusion. Nature *394*, 494–498.

Singer-Krüger, B., Frank, R., Crausaz, F., and Riezman, H. (1993). Partial purification and characterization of early and late endosomes from yeast. Identification of four novel proteins. J. Biol. Chem. *268*, 14376–14386.

Singer-Krüger, B., Nemoto, Y., Daniell, L., Ferro-Novick, S., and De Camilli, P. (1998). Synaptojanin family members are implicated in endocytic membrane traffic in yeast. J. Cell Sci. *111*, 3347–3356.

Spelbrink, R.G., and Nothwehr, S.F. (1999). The yeast *GRD20* gene is required for protein sorting in the *trans*-Golgi network/endosomal system and for polarization of the actin cytoskeleton. Mol. Biol. Cell *10*, 4263–4281.

Srinivasan, S., Seaman, M., Nemoto, Y., Daniell, L., Suchy, S.F., Emr, S., Decamilli, P., and Nussbaum, R. (1997). Disruption of three phosphatidylinositol-polyphosphate 5-phosphatase genes from *Saccharomyces cerevisiae* results in pleiotropic abnormalities of vacuole morphology, cell shape, and osmohomeostasis. Eur. J. Cell Biol. *74*, 350–360.

Stenmark, H., Aasland, R., Toh, B.H., and Darrigo, A. (1996). Endosomal localization of the autoantigen EEA1 is mediated by a zinc-binding FYVE finger. J. Biol. Chem. *271*, 24048–24054.

Stevens, T., Esmon, B., and Schekman, R. (1982). Early stages in the yeast secretory pathway are required for transport of carboxypeptidase Y to the vacuole. Cell *30*, 439–448.

Stolz, L.E., Huynh, C., Thorner, J., and York, J.D. (1998). Identification and characterization of an essential family of inositol polyphosphate 5-phosphatases (*INP53*, *INP52*, and *INP53* gene products) in the yeast *Saccharomyces cerevisiae*. Genetics *148*, 1715–1729.

Vater, C.A., Raymond, C.K., Ekena, K., Howald-Stevenson, I., and Stevens, T.H. (1992). The *VPS1* protein, a homolog of dynamin required for vacuolar protein sorting in *Saccharomyces cerevisiae*, is a GTPase with two functionally separable domains. J. Cell Biol. *119*, 773–786.

Wilcox, C.A., Redding, K., Wright, R., and Fuller, R.S. (1992). Mutation of a tyrosine localization signal in the cytosolic tail of yeast Kex2 protease disrupts Golgi retention and results in default transport to the vacuole. Mol. Biol. Cell *3*, 1353–1371.